Scattering Amplitudes in Quantum Electrodynamics at Infinite Energy, and Possible Implications for Hadron Physics*

SHAU-JIN CHANG AND PAUL M. FISHBANE
Physics Department, University of Illinois, Urbana, Illinois 61801
(Received 13 April 1970)

We study in pure quantum electrodynamics the scattering amplitudes at infinite energy due to multiphoton exchange, with interactions among the exchange photons. Such processes, elastic or inelastic, lead to logarithmic dependence on s. The $\ln s$ dependence is found to be associated with the invariance of subgraphs under a boost along the direction of the high-energy collision. Theoretically, our results lead towards a more efficient way of handling a large class of diagrams, and a better understanding of j-plane cut behavior. We speculate that several features of our results generalize to hadron physics. Among these are features in common with the limiting fragmentation hypothesis, and the appearance of pionization in a many-fireball structure. Finally, in the absence of radiative corrections, we demonstrate that the e^-, e^+ elastic scattering amplitude can be expressed as an eikonal form, with $\chi(\mathbf{b})$ being generated by the sum of all connected pieces.

I. INTRODUCTION

MANY theories have been proposed to describe high-energy hadron scattering at large s and finite t. Among these are the Regge model and the droplet model[1]; the droplet model is related to the eikonal[2] and diffraction models. Recently, the droplet model was generalized to qualitatively describe the inelastic processes as well. In particular, a theory of limiting fragmentations was proposed.[3] Each of these models has some experimental support. At present, it is not clear whether one can single out a model which is applicable to all processes.

These models are partially built on extrapolations from nonrelativistic potential scattering theory instead of relativistic first principles. It is of great interest to know if these models can be understood through relativistic field-theory calculations. Some progress has already been made along this line. For example, Regge behavior was shown to appear in a $\lambda\phi^3$ theory when ladder diagrams in the t channel are summed.[4] Recently, Cheng and Wu[5] showed that the forward elastic electron-electron (positron), electron-photon, and photon-photon scattering amplitudes in quantum electrodynamics with two-photon exchange at large s increase linearly like $sf(t)$ at fixed t. This result was generalized to include multiphoton exchange processes.[6] It was shown that the eikonal form emerges naturally when all possible crossed ladder diagrams in the s channel are summed.[6–8] We feel that it is important to associate simple physical features with special sets of diagrams. Thus, one may hope to construct a more complete theory which encompasses more of the observed features of high-energy collisions.

This paper deals with the high-energy behavior of a large class of diagrams in quantum electrodynamics (QED). A particular kind of diagram we study is shown in Fig. 1(a). We are interested in the limit of large s and finite t. The signaling feature of such diagrams is that they do not have pure photon states in the t channel. This is to be compared with pure photon-exchange diagrams, which behave like $sf(t)$. We shall see in general that at large s and finite t the diagrams we studied contribute logarithmic factors of s. The derivation from pure $sf(t)$ behavior is consistent with previous work of Gribov and Pomeranchuk,[9] who showed on the general grounds of unitarity in the t channel that $sf(t)$ cannot be the true asymptotic behavior of the elastic amplitude for positive t. Their argument can be understood in the t-channel partial-wave decomposition in which the expression $sf(t)$ implies a fixed pole at $j=1$. This fixed pole leads to difficulty with elastic unitarity:

$$\mathrm{Im}A_j(t) = -|A_j(t)|^2. \tag{1.1}$$

Because the right-hand side of (1.1) has a double pole at $j=1$ while the left-hand side has only a single pole, we are led to an accumulation of poles or essential singularity at $j=1$. It was suggested that t-channel unitarity might also imply the existence of a branch point. Then, a cut which would put the essential singularity on an unphysical sheet would be a satisfac-

* Work supported in part by the National Science Foundation under Contract No. NSF GP 19433.

[1] T. T. Chou and C. N. Yang, Phys. Rev. **170**, 1591 (1968); **175**, 1832 (1968).

[2] R. J. Glauber, in *Lectures in Theoretical Physics*, edited by W. E. Britten and L. G. Dunham (Interscience, New York, 1959), Vol. 1.

[3] J. Benecke, T. T. Chou, C. N. Yang, and E. Yen, Phys. Rev. **188**, 2159 (1969).

[4] B. W. Lee and R. F. Sawyer, Phys. Rev. **127**, 2266 (1962).

[5] H. Cheng and T. W. Wu, Phys. Rev. Letters **22**, 666 (1969); Phys. Rev. **182**, 1852 (1969); **182**, 1868 (1969); **182**, 1873 (1969); **182**, 1899 (1969).

[6] S. J. Chang and S. Ma, Phys. Rev. Letters **22**, 1334 (1969); Phys. Rev. **188**, 2385 (1969); H. Cheng and T. T. Wu, *ibid.* **186**, 1611 (1969).

[7] H. D. I. Abarbanel and C. Itzykson, Phys. Rev. Letters **23**, 53 (1969); F. Englert *et al.*, Nuovo Cimento **64A**, 561 (1969); M. Lévy and J. Sucher, Phys. Rev. **186**, 1656 (1969).

[8] See also the earlier work of M. Lévy, Phys. Rev. **130**, 791 (1963); R. Torgerson, *ibid.* **143**, 1194 (1966). These two authors showed that the *ee* elastic amplitude behaves like $sf(t)$ and is consistent with the eikonal form up to sixth order in e.

[9] V. N. Gribov and I. Ya Pomeranchuk, Phys. Letters **2**, 239 (1962).

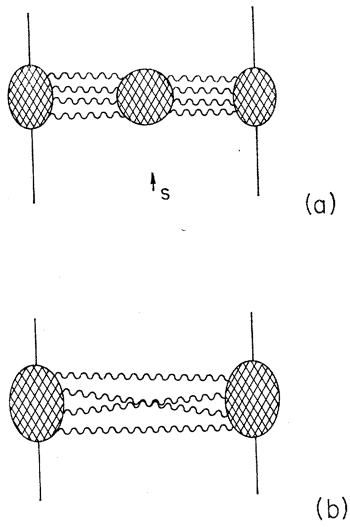

FIG. 1. (a) General class of diagrams considered in this paper at large s and small t. The bubble in the middle represents interactions of the exchanged photons. (b) Simpler multiphoton exchange diagram, which has been previously studied.

tory solution to this problem.[10] Such a branch point would modify the simple power behavior in s, characteristic of Regge poles, to include logarithmic dependence.

The t-channel iteration of two (e.g.) multiphoton processes, as in Fig. 1(b), leads to processes with one (e.g.) bubble in the middle, joining to the initial and final particles by exchange photons. From the above arguments, one might expect that Fig. 1(a) might give logarithmic dependence on s at large s. Indeed, it was shown in Ref. 11 that the lowest-order bubble diagrams, Fig. 2, of a charged scalar-meson theory lead to an amplitude with $s \ln s$ dependence. It was mentioned in this reference that the individual diagrams actually behave like s^2 at large s. The cancellation and final $s \ln s$ dependence come about in a way that is not obvious. A similar calculation was carried out recently by Frolov, Gribov, and Lipatov[12] in quantum electrodynamics, with similar $s \ln s$ dependence.

One of the purposes of this paper is to give a natural explanation of this $\ln s$ dependence, and to extend and refine the consequences of diagrams of the type of Fig. 1(a). We shall discuss the general characteristics of such diagrams, including more qualitative discussions of their t-channel iteration and multiple exchange.

A few of the possible generalizations of our result to hadron physics are the following. (a) For elastic scattering, we find the presence of $\ln s$ factors in the amplitude. Since QED is a more realistic theory than $\lambda\phi^3$, our results might lead to a more realistic way to calculate the effects of cuts and the nature of the Pomeranchon.[13] (b) We may divide inelastic scattering into two categories. In the first category, inelastic products are formed at the external vertices. In our model, it is natural that such diagrams factor and become independent of s. This picture has much in common with the hypothesis of limiting fragmentation[3] recently proposed by Benecke, Chou, Yang, and Yen. Extra $\ln s$ factors are again introduced into the amplitude by bubbles in the middle. In the second category, the bubbles "evaporate" particles at low momentum in the rest frame of the bubble. These are so-called "pionization"[14] products. This picture, which is consistent with, but not required by, limiting fragmentation, is a picture of a hierarchy of "fireballs,"[14] separated energetically from one another by terms depending on $\ln s$. In particular, the number of such fireballs grows like $\ln s$, giving multiplicity of final particles which grows naturally like $\ln s$. Of course, an actual inelastic process will be a combination of these categories.

Our paper is summarized as follows: In Sec. II we give the kinematics and general formulation of diagrams of type of Fig. 1(a) for the elastic process in quantum electrodynamics. In Sec. III we discuss the lowest-order bubble in detail, finding a result which agrees with that of Frolov *et al.*[12] In Sec. IV we extend our results to other types of bubbles. In Sec. V we briefly discuss multiple exchange of bubbles, and the characteristics of the resulting eikonalization. The general considerations are extended in Sec. VI to include multiparticle production processes. In Sec. VII we discuss t-channel iteration and the possible consequences of our results for hadron physics. In the Appendix, the general eikonalization for s-channel iteration of a "connected piece" is derived.

II. KINETICS AND GENERAL FORMULATION

In this section we want to show how the appropriate use of infinite-momentum techniques at high energy can simplify a scattering problem. In particular, we shall show that it is possible to remove over-all s

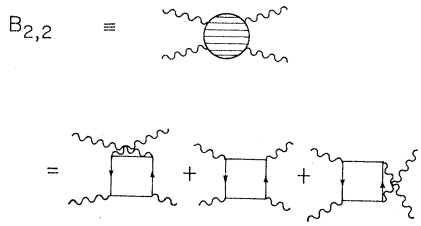

FIG. 2. Simplest two-photon → two-photon bubble, consisting only of a fermion loop. Gauge invariance requires the consideration of the three Feynman diagrams shown.

[10] See, e.g., *Proceedings of the 1969 Regge Cut Conference*, edited by P. M. Fishbane and L. M. Simmons (Univ. of Wisconsin, Madison, 1969).

[11] H. Cheng and T. T. Wu, Phys. Rev. Letters **22**, 1405 (1969).

[12] G. V. Frolov, V. N. Gribov, and L. N. Lipatov, Phys. Letters **31B**, 34 (1970).

[13] For an earlier attempt at this problem, see M. Gell-Mann, M. L. Goldberger, and F. E. Low, Rev. Mod. Phys. **36**, 640 (1964).

[14] See M. Koshiba, in *Proceedings of the Third International Conference on High-Energy Collisions* (Gordon and Breach, New York, 1969). A summary of the latest progress in cosmic-ray physics can be found in the *Proceedings of the Tenth International Conference on Cosmic Rays* [Can. J. Phys. **46**, No. 10, Pts. 2–4 (1968)].

dependence up to logarithmic terms. When a scattering process proceeds by exchange of more or less complicated units, there is a natural kind of factorization which simplifies this problem. We shall first concentrate on elastic scattering with exchange of the "bubble" shown in Fig. 3(a), but we shall also indicate in this section how our formulation generalizes.

We want to consider an elastic process in QED. For our specific example, we consider e^-e^- scattering with two-photon exchange as in Fig. 3. The cross-hatched blobs along the electron lines include all possible radiative corrections, while the cross-hatched bubble in the middle of the diagram describes photon-photon scattering for off-mass-shell photons. Although it is not necessary for the general features described in this section, we would like to make here the distinction between "primitive" and "nonprimitive" bubbles. We define a primitive bubble as one which cannot be separated into two bubbles by cutting internal photon lines only. This definition is illustrated graphically by Fig. 3(b). The distinction is important in extracting the particular behavior in $\ln s$ arising from the photon-photon scattering.

The scattering amplitude for the process shown in Fig. 3(a) is

$$M=\int A_{\alpha\beta}(p_a,p)B_{\alpha\beta;\mu\nu}(p,q)C_{\mu\nu}(q,p_c)\times\frac{ie^2}{p_1^2-\mu^2+i\epsilon}\frac{ie^2}{p_2^2-\mu^2+i\epsilon}\frac{ie^2}{q_1^2-\mu^2+i\epsilon}\frac{ie^2}{q_2^2-\mu^2+i\epsilon}\times\frac{d^4p}{(2\pi)^4}\frac{d^4q}{(2\pi)^4}, \quad (2.1)$$

where p_1, p_2, q_1, and q_2 are four-momenta of the exchange photons. $A_{\alpha\beta}$ and $C_{\mu\nu}$ are the partial amplitudes for the blobs associated with the colliding particles a and c, while $B_{\alpha\beta;\mu\nu}$ is the partial amplitude associated with the photon-photon scattering bubble. μ is a fictitious photon mass.[15] In the center-of-mass frame, the 1-2 plane is defined by the momentum transfer $\mathbf{k}\equiv(k^1,k^2)$. If $\mathbf{P}=\frac{1}{2}(\mathbf{p}_{ai}+\mathbf{p}_{af})$, the average momentum of particle a, lies in the plus-z direction of magnitude P, then

$$\begin{aligned}\mathbf{p}_{ai}&=\mathbf{P}-\tfrac{1}{2}\mathbf{k}, \qquad \mathbf{p}_{af}=\mathbf{P}+\tfrac{1}{2}\mathbf{k},\\ \mathbf{p}_{ci}&=-\mathbf{P}+\tfrac{1}{2}\mathbf{k}, \quad \mathbf{p}_{cf}=-\mathbf{P}-\tfrac{1}{2}\mathbf{k}.\end{aligned} \quad (2.2)$$

For very large incident energy ($\sim P$) and finite $k=|\mathbf{k}|$, the conventional invariant variables are

$$s\approx(2P)^2, \quad t=-k^2. \quad (2.3)$$

In this paper we are, in fact, only interested in the asymptotic behavior of the amplitude in the limit of large s but finite t.

We now turn to the question of the convenient frame for the evaluation of various pieces of the amplitude. The general principle involved is that it is most convenient to boost to a frame in which the appropriate variables are finite as $s\to\infty$, as was discussed at some length in Ref. 16. For example, let us consider $A_{\alpha\beta}(p_a,p)$. The appropriate frame for studying this quantity is a frame which moves along the three-axis with particle a, called the "standard frame" for particle a. This frame is characterized in the infinite-momentum language[16] by

$$\begin{aligned}&p_{a+}'\equiv p_a'^0+p_a'^3=e^{-\lambda}p_{a+}=1, \quad e^\lambda\approx\sqrt{s}\\ &\mathbf{p}_a'=\mathbf{p}_a,\\ &p_{a-}'\equiv p_a'^0-p_a'^3=e^{\lambda}p_{a-}=\mathbf{p}_a'^2+m^2,\end{aligned} \quad (2.4)$$

where boldface vectors are now always vectors in the 1-2 plane. The form for p_{a-}' comes from the mass-shell condition for particle a, where $p_a'^2=m^2$ is the electron mass squared. By construction, the new variables p_a' remain finite as $s\to\infty$. In this frame, p transforms to

$$\begin{aligned}&p_+'=p_+/\sqrt{s}=p_+/p_{a+},\\ &\mathbf{p}'=\mathbf{p},\\ &p_-'=(\sqrt{s})p_-.\end{aligned} \quad (2.5)$$

For those readers not familiar with the infinite-momentum boost techniques, the transformation defined by Eq. (2.4) [or (2.5)] may be regarded as a *scale transformation* whose sole purpose is to make the final integration variables p' finite at $s=\infty$. In particular, p_+' has the simple physical meaning of the fraction of the total longitudinal momentum p_{a+} going into the photons, p_+/p_{a+}. It is known that this is a convenient parametrization for the description of high-energy scattering.

Now we can express $A_{\alpha\beta}(p_a,p)$ in terms of p_a' and p'. This is trivial, because $A_{\alpha\beta}$ transforms like a tensor:

$$\begin{aligned}&A_{++}(p_a,p)=sA_{++}(p_a',p'),\\ &A_{+\perp}(p_a,p)=(\sqrt{s})A_{+\perp}(p_a',p'), \quad \perp=1,2\\ &A_{+-}(p_a,p)=A_{+-}(p_a',p'),\\ &A_{-\perp}(p_a,p)=(1/\sqrt{s})A_{-\perp}(p_a',p'),\\ &A_{--}(p_a,p)=(1/s)A_{--}(p_a',p'), \quad \ldots .\end{aligned} \quad (2.6)$$

Notice that $A(p_a',p')$ remains finite as $s\to\infty$, whereas in the c.m. frame $A(p_a,p)$ becomes infinite. This change of variables performs the very important service of explicitly removing s dependence.

Similarly, we want to study $C_{\mu\nu}(q,p_c)$ in the standard frame of particle c. Since particle c has a large minus component and small plus component, take as new

[15] This fictitious photon mass reminds us that we must still treat renormalization properly. We treat this in the standard way. Evaluate the answer by first introducing proper regulators and counter terms, then letting the regulator masses $M\to\infty$. The result is independent of M and is the final answer with renormalization taken into account.

[16] S. J. Chang and S. Ma, Phys. Rev. **180**, 1506 (1969); **188**, 2385 (1969); thereafter referred to as I and II.

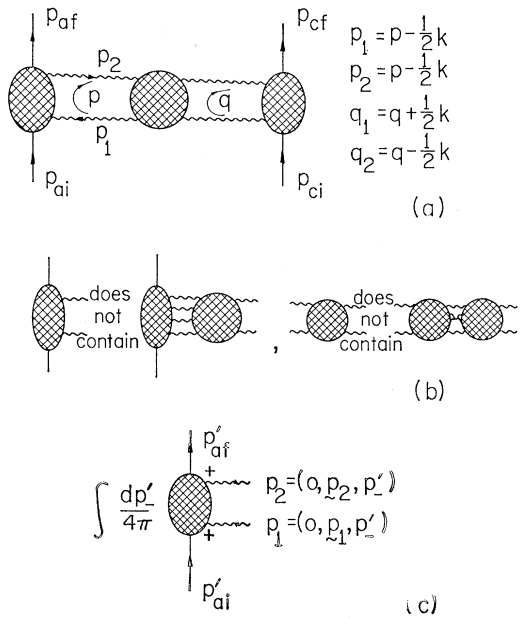

FIG. 3. (a) Fermion-fermion scattering with two exchanged photons interacting once, i.e., with a single bubble. The cross-hatched blobs are primitive, by which we mean that they contain no pure photon states in the t channel. This is illustrated in (b) for the vertex blob and the bubble in the middle. (c) shows the left-hand vertex blob isolated in its standard frame. Note that the exchange photon lines have no plus component.

variables

$$p_{c-}''=1, \quad \mathbf{p}_c''=\mathbf{p}_c, \quad p_{c+}''=\mathbf{p}_c^2+m^2 \tag{2.7}$$

and

$$q_-''=(1/\sqrt{s})q_-, \quad \mathbf{q}''=\mathbf{q}, \quad q_+''=(\sqrt{s})q_+. \tag{2.8}$$

The leading part of the tensor $C_{\mu\nu}$ is

$$C_{--}(q,p_c)=sC_{--}(q'',p_c''). \tag{2.9}$$

$C_{--}(q'',p_c'')$ remains finite as $s\to\infty$.

Since A_{++} and C_{--} are larger by $\sqrt{s}$ than other components, the only components of the bubble in the middle we need to consider in the $s\to\infty$ limit are $B_{--;++}(p,q)$. The original c.m. variables p and q are most suitable for describing B.

We have thus seen that the natural variables for describing different pieces of the partial amplitudes are scaled differently in the + and − components. Transverse momentum variables are scaled in the same way in all these reference frames. For instance, we have seen that $A_{\alpha\beta}$ is best described by the finite variables p_a' and p' (i.e., p_a and p in the standard frame of particle a), while $C_{\mu\nu}$ should be described by q'' and p_c'' (i.e., q and p_c in the standard frame of particle c). From the analysis of lower-order calculations, one finds that the dominant contribution to the amplitude comes from the integration regions where all these naturally scaled variables are finite. Thus p_a' and p' are finite in the standard frame a, p and q are finite in the c.m. frame (this point will be discussed in detail later), and q'' and p_c'' are finite in the standard frame c. However, one knows that the variables in different regions are the same momentum variables scaled differently. For example, p_-' in the standard frame a is related to the c.m. variable p_- through $p_-=(1/\sqrt{s})p_-'$. Hence, a finite p_-' in the standard frame a leads to a small $p_-=O(1/\sqrt{s})$ in the c.m. frame. Conversely, a finite p_+ in the c.m. frame implies a small $p_+'=O(1/\sqrt{s})$ in the standard frame.

As $s\to\infty$, we may ignore the $O(1/\sqrt{s})$ terms and replace all the small variables, p_+', p_-, q_+, and q_-'', by zeros. We have checked explicitly in lower-order diagrams that the neglect of these $1/\sqrt{s}$ terms does not affect the leading term in the amplitudes. In complicated diagrams in which a direct verification is not at present possible, we justify ignoring these $1/\sqrt{s}$ terms by requiring that the remaining integrals be finite and s independent. The full amplitude is finally described by the remaining set of finite integration variables $\mathbf{p}$, $\mathbf{q}$, p_-', p_+, q_-, and q_+'' and by the finite external variables p_a' and p_c''. The remaining variables p_+', p_-, q_+, and q_-'' are small $[O(1/\sqrt{s})]$ and are replaced by zero. In terms of the finite variables, the volume factors in momentum space are

$$\begin{aligned}\frac{d^4p}{(2\pi)^4}&=\frac{1}{2(2\pi)^4\sqrt{s}}(dp_+dp_-'d^2\mathbf{p}),\\ \frac{d^4q}{(2\pi)^4}&=\frac{1}{2(2\pi)^4\sqrt{s}}(dq_+''dq_-d^2\mathbf{q}).\end{aligned} \tag{2.10}$$

The photon propagators are, in terms of the new variables,

$$\begin{aligned}\frac{-i}{p^2-\mu^2+i\epsilon}&=\frac{-i}{(p_+p_-')/\sqrt{s}-\mathbf{p}^2-\mu^2+i\epsilon}\\ &=\frac{i}{\mathbf{p}^2+\mu^2+O(1/\sqrt{s})},\\ \frac{-i}{q^2-\mu^2+i\epsilon}&=\frac{i}{\mathbf{q}^2+\mu^2+O(1/\sqrt{s})}.\end{aligned} \tag{2.11}$$

We shall ignore the $O(1/\sqrt{s})$ terms in the exchange photon propagators. This is equivalent to ignoring the contribution of the potential poles in our calculations. It is known from explicit lower-order calculations (up to e^6)[17] that the potential poles do not contribute if diagrams with photons permuted in all possible ways are included. Whether this is true to all orders in e^2 and in all possible bubble diagrams is not known. We shall assume it is true in this paper; we hope to study this point more carefully in the future.

[17] The cancellation of potential poles in $\lambda\phi^3$ theory and in QED was shown by A. N. Chester, Phys. Rev. **140**, B85 (1965); R. Torgerson, *ibid.* **143**, 1194 (1966).

Putting everything together, we find that Eq. (2.1) becomes

$$M=\tfrac{1}{4}s\int A_{++}(p_a',p')\frac{dp_-'}{4\pi}\int\frac{dp_+}{4\pi}\frac{dq_-}{4\pi}B_{--;++}(p,q)\times\int C_{--}(q'',p_c'')\frac{dq_+''}{4\pi}\frac{d^2p}{(2\pi)^2}\frac{d^2q}{(2\pi)^2}\times\frac{-ie^2}{\mathbf{p}_1^2+\mu^2}\frac{-ie^2}{\mathbf{p}_2^2+\mu^2}\frac{-ie^2}{\mathbf{q}_1^2+\mu^2}\frac{-ie^2}{\mathbf{q}_2^2+\mu^2},\quad(2.12)$$

where p, q are loop momenta, $p_1=p+\frac{1}{2}k$, $p_2=p-\frac{1}{2}k$, and $q_1=q+\frac{1}{2}k$, $q_2=q-\frac{1}{2}k$. For general $(M+N)$-photon exchange diagrams, when M, $N\geq 2$ as in Fig. 4, there are $(M+N)$ $\sqrt{s}$ factors from each large vertex and $(M+N-2)$ $1/\sqrt{s}$ factors from the loop integrals. Thus there is always a single s factor left over. (See also our discussion in Sec. IV.) Similarly, when any blob or bubble is broken up into primitive components, i.e., when primitive bubbles are iterated across a diagram, there is a single s factor over-all.

The advantage of using Eq. (2.12) rather than the original c.m. amplitude of Eq. (2.1) is that as $s\to\infty$ all the pieces of (2.12) become *separately* finite (except for possible logarithmic terms from the photon-photon scattering piece). Thus one can treat one factor at a time. This kind of factorization of the amplitudes into s-independent partial amplitudes is a general result. In the example we are studying, the first factor is

$$\int\frac{dp_-'}{4\pi}A_{++}(p_a',p').$$

A_{++} actually depends only on the transverse and minus components of p_a' and p'. The p_{a+}' is fixed equal to unity and p_+' is zero. In terms of the decomposition $p_\mu=(p_+,\mathbf{p},p_-)$, this first factor is represented graphically as in Fig. 3(c). This partial amplitude can be evaluated without knowing the $B_{--;++}$ or C_{--} parts. A similar conclusion applies to the $B_{--;++}$ and C_{--} factors. We shall refer to parts A_{++}, $B_{--;++}$, and C_{--} as kinematically decoupled.

The contribution due to the bubble in the middle,

$$\int\frac{dp_+}{4\pi}\frac{dq_-}{4\pi}B_{--;++},$$

leads to extra $\ln s$ factors as $s\to\infty$. In fact, a Regge cut, which would mean extra $\ln s$ factors, is required by the Gribov-Pomeranchuk theorem.[9] In particular, if all the cross-hatched blobs of Figs. 3(a) or 4 are primitive, a single $\ln s$ factor results, as we shall show in detail. The existence of the $\ln s$ term in the lowest-order box diagram of a charged scalar-meson theory was established by Cheng and Wu[11] through explicit calculation. In this paper, we wish to present a simple physical reason why this s $\ln s$ structure emerges naturally for *all* single primitive bubble diagrams, and its coefficient can be identified straightforwardly.

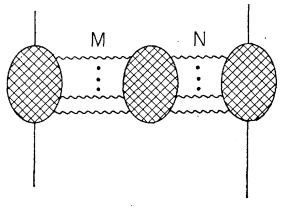

FIG. 4. Single-bubble diagram with M photons attaching from one side and N from the other. $M+N$ must be even.

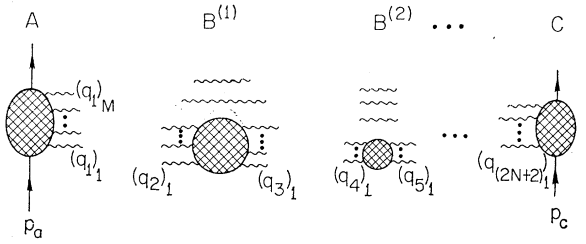

FIG. 5. Multiple-bubble diagram for fermion-fermion scattering. Note that not all the photon lines attach to every bubble, all of which are taken to be primitive here.

The extra $\ln s$ factor in our calculation is related to the invariance property of the bubble amplitude $B_{--;++}$ under acceleration along the three-axis. This invariance property implies that the integrated bubble amplitude contains a longitudinal phase-space factor $\ln s$ in the K^3 boost space. One can see that this technique is applicable to many-bubble processes as well as to the inelastic processes. We shall discuss these points in detail in Secs. III and IV.

The factorization of the amplitude into finite (up to factors of $\ln s$) kinematically decoupled parts is quite general. To apply this to an N-bubble case, as in Fig. 5, let us use the convention that the bubbles are drawn from right to left according to increasing values of the plus component of the electron loop momenta p_+. This kind of representation makes sense only at very large s (hence very large $\ln s$), when separation between bubbles in $\ln p_+$ space is larger than the extent of the bubbles themselves in this space. (When bubbles are primitive, they have only finite extension in the $\ln p_+$ space.[18] Thus it is sensible at this stage to demand that all bubbles be primitive. This fixed the logarithmic dependence that a single bubble contributes as $\ln s$.)

For the above graphical representation, and for terms leading in $\ln s$, photons attaching from the *right* to a bubble have coupling γ_+ and photons attaching from the *left* to a bubble have coupling γ_-. Any diagrams with a wrong plus or minus γ matrix at a vertex is at least an order of $\ln s$ smaller. This can be verified from the Lorentz transformation laws of the bubbles. Dia-

[18] This can be seen in two ways. First, we find from explicit calculation (see Sec. III) that the primitive bubble amplitude by itself is finite and does not contain further logarithmic divergence. Second, as was shown in Refs. 6 and 8, the only leading diagrams for large subenergy are those which can be separated into two parts by cutting only photon lines.

grams belonging to the same Feynman diagram but with different ordering in the $\ln p_+$ space (see Fig. 6) must be counted as different diagrams in our representation. This is analogous to Weinberg's infinite-momentum rules,[19] where different time orderings of a single Feynman diagram are taken to be distinct diagrams.

Keeping the above remarks in mind, we can express the scattering diagram of Fig. 5 for N primitive bubbles as

$$M=\frac{1}{2^{N+1}}\int A_{++\cdots+}(p_a,\{q_1{}^i\})\Big(\prod_i\frac{dq_{1-}{}^i}{4\pi}\Big)4\pi\delta(\sum_i q_{1-}{}^i)$$
$$\times\int B_{--\cdots-,++\cdots+}{}^{(1)}(\{q_2{}^i\},\{q_3{}^j\})\Big(\prod_{i,j}\frac{dq_{2+}{}^i}{4\pi}\frac{dq_{3-}{}^j}{4\pi}\Big)$$
$$\times 4\pi\delta(\sum_i q_{2+}{}^i)4\pi\delta(\sum_j q_{3-}{}^j)\cdots$$
$$\times\int C_{--\cdots-}(\{q_{2N+2}{}^i\},p_c)\Big(\prod\frac{dq_{(2N+2)+}{}^i}{4\pi}\Big)$$
$$\times 4\pi\delta(\sum_i q_{(2N+2)-}{}^i)\prod_{\text{(all internal photons)}}\Big(\frac{-ie^2}{\mathbf{q}^2+\mu^2}\frac{d^2q}{(2\pi)^2}\Big)$$
$$\times(2\pi)^2\delta^{(2)}(\sum\mathbf{q}-\mathbf{k}),\quad(2.13)$$

where all p's are q's are c.m. variables. The subscripts $2n$, $2n+1$ label all photons associated with the nth bubble, and superscript i (and j) describes the ith (and jth) photon in the above group(s) of photons. In deriving the above result, we make use of the fact that the leading term in $B_{\cdots,\mu\nu\cdots}{}^{(n)}B_{\mu\nu,\cdots}{}^{(n+1)}$, for instance, is $(\frac{1}{2})^2B_{\cdots,++\cdots}{}^{(n)}B_{--\cdots,\cdots}{}^{(n+1)}$. The natural variables for the nth bubble are, in analogy to the one-bubble case,

$$q_+{}^{(2n)\prime}=(\sqrt{s_n})q_+{}^{(2n)},\qquad \mathbf{q}^{(2n)\prime}=\mathbf{q}^{(2n)},$$
$$q_-{}^{(2n)\prime}=(1/\sqrt{s_n})q_-{}^{(2n)},\quad q_+{}^{(2n+1)\prime}=(\sqrt{s_n})q_+{}^{(2n+1)},$$
$$\mathbf{q}^{(2n+1)\prime}=\mathbf{q}^{(2n+1)},\qquad q_-{}^{(2n+1)\prime}=(1/\sqrt{s_n})q_-{}^{(2n+1)},\quad(2.14)$$

where $\sqrt{s_n}$ is the typical plus component of the nth bubble measured in the c.m. frame. The dominant contribution of the nth bubble comes from the integration region where the variables $q^{(2n)\prime}$, $q^{(2n+1)\prime}$ are finite. The $\{s_n\}$ satisfy[20]

$$\sqrt{s}\gg\sqrt{s_1}\gg\sqrt{s_2}\gg\cdots\gg\sqrt{s^N}\gg m^2/\sqrt{s}.\quad(2.15)$$

After ignoring terms of order $O((s_{n+1})/s_n)$ or $O(1/\ln s)$ smaller, we have

$$q_\mu{}^{(2n)\prime}=[q_+{}^{(2n)\prime},\mathbf{q}^{(2n)},0],$$
$$q_\mu{}^{(2n+1)\prime}=[0,\mathbf{q}^{(2n+1)},q^{(2n+1)\prime}].\quad(2.16)$$

[19] S. Weinberg, Phys. Rev. **150**, 1313 (1966).

[20] Equivalently, if we call $\sqrt{s_n}'$ the typical minus component of the nth bubble in the c.m. system, then $\sqrt{s_n}'$ increases as n increases. In studying iterations of the Mandelstam cut diagram, P. V. Landshoff and J. C. Polkinghorne [Phys. Rev. **181**, 1989 (1969)] similarly discovered the usefulness of standard frames for studying a t-channel iterated exchange process. They also find that use of these variables leads naturally to $\ln s$ dependence.

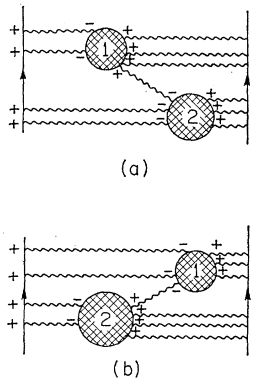

FIG. 6. Two connected two-bubble diagrams of the same order in the coupling. In our kinematic region the side from which a photon attaches to a bubble is important, so that (a) and (b) represent not a single diagram, but two diagrams which must be considered separately.

We now transform the bubble contributions to each of their respective finite frames. For each of the + (or −) tensor indices we pick up a factor $\sqrt{s_n}$ (or $1/\sqrt{s_n}$) from this transformation. For each of the integration variables $dq_-{}^{(n)}=(1/\sqrt{s_n})dq_-{}^{(n)\prime}$ (or $dq_+{}^{(n)}$), we have a factor $1/\sqrt{s_n}$ (or $\sqrt{s_n}$). Putting all these factors together, we find that all intermediate $\sqrt{s_n}$ factors cancel. The only factors remaining are one $\sqrt{s}$ from bubble A and one $\sqrt{s}$ from bubble C, giving

$$M=\frac{s}{2^{N+1}}\int A_{++\cdots+}(p_a',\{q_{1-}{}^i\}')\Big(\prod_i\frac{dq_{1-}{}^{i\prime}}{4\pi}\Big)4\pi\delta(\sum_i q_{1-}{}^{i\prime})$$
$$\times\int B_{--\cdots-;++\cdots+}{}^{(1)}(\{q_{2+}{}^{i\prime}\},\{q_{3-}{}^{j\prime}\})\Big(\prod_{i,j}\frac{dq_{2+}{}^{i\prime}}{4\pi}\frac{dq_{3-}{}^{j\prime}}{4\pi}\Big)$$
$$\times 4\pi\delta(\sum_i q_{2+}{}^{i\prime})4\pi\delta(\sum_j q_{3-}{}^{j\prime})\cdots$$
$$\int C_{--\cdots-}(\{q_{(2N+2)+}{}^i\},p_c'')\Big(\prod_{i,j}\frac{dq_{(2N+2)+}{}^{i\prime}}{4\pi}\Big)$$
$$\times 4\pi\delta(\sum_i q_{(2N+2)+}{}^{i\prime})\prod_{\text{(all internal photons)}}\Big(\frac{-ie^2}{\mathbf{q}^2+\mu^2}\frac{d^2q}{(2\pi)^2}\Big)$$
$$\times(2\pi)^2\delta^{(2)}(\sum\mathbf{q}-\mathbf{k}).\quad(2.17)$$

The dependence of the functions A, $B^{(n)}$, ..., C on the transverse momenta has been suppressed. Note that in Fig. 5 not all the photons emitted from A are necessarily connected to B. Also note that as in Eq. (2.13), a four-dimensional δ function $4\pi\delta(\sum q_+)4\pi\delta(\sum q_-)(2\pi)^2\times\delta(\sum\mathbf{q}-\mathbf{k})$ must always be included between two bubbles. The effects of this δ function were already taken into account in writing Eq. (2.1) for a single two-photon → two-photon bubble.

As we shall explain in Sec. V, an N-bubble diagram will, in general, give rise to a factor $(\ln s)^N$. This factor is, of course, very important in analyzing and summing repeated bubbles. Finally, the generalization of the work of this section from elastic processes to inelastic processes is sketched in Sec. VI.

III. LOW-ORDER CALCULATION

In Sec. II, we mentioned that the $s\ln s$ dependence of the amplitudes emerges naturally if one realizes that

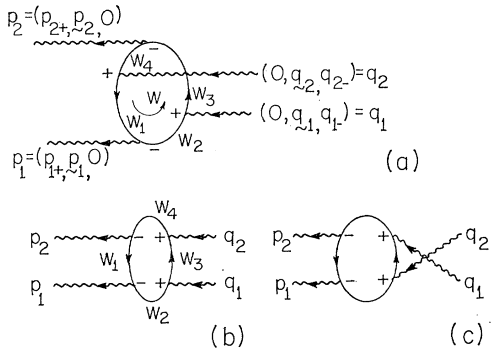

FIG. 7. The two-photon → two-photon bubble of Fig. 2 labeled carefully. Note that the p_- are zero as are the q_+.

the factor $\ln s$ reflects the longitudinal phase-space factor in the $\ln p_+$ space. In the following, we shall develop the technique in detail and work out the lowest-order contribution explicitly.

The contribution for a general bubble of Fig. 7 is (the integration over transverse momenta is omitted)

$$\int \frac{dp_+}{4\pi}\frac{dq_-}{4\pi} B_{--,++}(p,q), \tag{3.1}$$

where

$$\begin{aligned} &p_i=(p_{i+},\mathbf{p}_i,0), \quad p_{2+}=-p_{1+}\equiv p_+, \\ &q_i=(0,\mathbf{q}_i,q_{i-}), \quad q_{2-}=-q_{1-}\equiv -q_-, \quad i=1,2. \end{aligned} \tag{3.2}$$

Lorentz covariance implies that

$$B_{--,++}(e^{\lambda}p_+,e^{-\lambda}q_-;\,\mathbf{p},\mathbf{q})=B_{--,++}(p_+,q_-;\,p,q). \tag{3.3}$$

Hence $B_{--,++}$ can only be a function of p_+q_- and $(\mathbf{p},\mathbf{q})$,

$$B_{--,++}(p_+,q_-;\,\mathbf{p},\mathbf{q})=B_{--,++}(p_+q_-;\,\mathbf{p},\mathbf{q}). \tag{3.4}$$

Then,

$$\begin{aligned} &\int \frac{dp_+}{4\pi}\frac{dq_-}{4\pi}B_{--,++}(p,q) \\ &\quad=\int \frac{dp_+}{4\pi p_+}\frac{d(p_+q_-)}{4\pi}B(p_+q_-;\,\mathbf{p},\mathbf{q}) \\ &\quad=\int \frac{dp_+}{4\pi p_+}\int \frac{d(p_+q_-)}{4\pi}B(p_+q_-;\,\mathbf{p},\mathbf{q}). \end{aligned} \tag{3.5}$$

The second factor is independent of p_+, and can be worked out explicitly. It is a finite factor, which we shall work out further below. The $\int dp_+/p_+$ term diverges logarithmically. However, we have to recognize that as $p_+\sim\sqrt{s}$, i.e., as p_+ is comparable to $(p_a)_+$, there is a natural cutoff emerging from the A_{++} part of the amplitude. Similarly, as $p_+\sim 1/\sqrt{s}$, a cutoff is supplied by the C_{--} part of the amplitude. Hence, $\int dp_+/p_+$ no longer diverges, and yields

$$\int \frac{dp_+}{p_+}\approx 2\int_{1/\sqrt{s}}^{\sqrt{s}}\frac{dp_+}{p_+}=2\ln s, \tag{3.6}$$

where the factor 2 comes from the fact that p_+ can be both positive and negative. In analogy to the volume factor appearing in the usual calculation of the transition probability, the $\ln s$ factor reflects the translational invariance of the bubble amplitude in the $\ln p_+$ space. (We discuss this point further in Sec. VI.)

To see how our argument works in practice, we compute the $s\ln s$ term for the lowest-order box diagram of spinor QED. The calculation of other high-order bubbles will be briefly sketched.

For the box diagram 7(a), the amplitude is

$$\begin{aligned} B_{\mu\nu,\lambda\sigma}{}^{(a)}&=-\int\frac{d^4W}{(2\pi)^4}\mathrm{Tr}[S_F(W_1)\gamma_\nu S_F(W_2)\gamma_\sigma \\ &\quad\times S_F(W_3)\gamma_\mu S_F(W_4)\gamma_\lambda] \\ &=-\int\frac{d^4W}{(2\pi)^4}\mathrm{Tr}[(W_1+m)\gamma_\nu(W_2+m)\gamma_\sigma \\ &\quad\times(W_3+m)\gamma_\mu(W_4+m)\gamma_\lambda] \\ &\quad\times(D_1D_2D_3D_4)^{-1}, \end{aligned} \tag{3.7}$$

where

$$\begin{aligned} &D_j=W_j{}^2-m^2+i\epsilon, \quad j=1,2,3,4 \\ &W_1=W+p_1, \quad W_2=W, \quad W_3=W+q_1, \\ &\qquad W_4=W+q_1-p_2=W-q_2+p_1, \\ &p_i=(p_{i+},\mathbf{p}_i,0), \quad q_i=(0,\mathbf{q}_i,q_{i-}), \end{aligned} \tag{3.8}$$

and $p_1+p_2=q_1+q_2=(0,\mathbf{k},0)$.

The leading contribution corresponds to $\mu=\nu=-$, $\lambda=\sigma=+$, and gives

$$\begin{aligned} B_{--,++}{}^{(a)}(p,q)&=-\int\frac{d^4W}{(2\pi)^4} \\ &\quad\times\mathrm{Tr}[(W_1+m)\gamma_-(W_2+m)\gamma_+ \\ &\quad\times(W_3+m)\gamma_-(W_4+m)\gamma_+](D_1D_2D_3D_4)^{-1}. \end{aligned} \tag{3.9}$$

Since $\gamma_+{}^2=\gamma_-{}^2=0$, we have

$$\begin{aligned} \gamma_+(W+m)\gamma_-&=\gamma_+(-\boldsymbol{\gamma}\cdot\mathbf{W}+m)\gamma_- \\ &=\gamma_+\gamma_-(\boldsymbol{\gamma}\cdot\mathbf{W}+m), \\ \gamma_-(W+m)\gamma_+&=\gamma_-(-\boldsymbol{\gamma}\cdot\mathbf{W}+m)\gamma_+. \end{aligned} \tag{3.10}$$

Hence, the trace (the numerator $N^{(a)}$) reduces to

$$\begin{aligned} N^{(a)}&=8\,\mathrm{Tr}[(m+\boldsymbol{\gamma}\cdot\mathbf{W}_1)(m-\boldsymbol{\gamma}\cdot\mathbf{W}_2)(m+\boldsymbol{\gamma}\cdot\mathbf{W}_3) \\ &\qquad\times(m-\boldsymbol{\gamma}\cdot\mathbf{W}_4)] \\ &=32[(\mathbf{W}_1\cdot\mathbf{W}_2+m^2)(\mathbf{W}_3\cdot\mathbf{W}_4+m^2) \\ &\quad+(\mathbf{W}_1\cdot\mathbf{W}_4+m^2)(\mathbf{W}_2\cdot\mathbf{W}_3+m^2) \\ &\qquad-(\mathbf{W}_1\cdot\mathbf{W}_3+m^2)(\mathbf{W}_2\cdot\mathbf{W}_4+m^2)]. \end{aligned} \tag{3.11}$$

The trace is a function of $\mathbf{W}$ only, and does not depend on W_+ or W_-. It is in fact quite straightforward to verify from (3.9) that $B_{--,++}{}^{(a)}$ is indeed a function of

p_+ and q_- only through the product p_+q_-. Note that $B^{(a)}$ is formally divergent after W integration. We shall see that the sum of $B^{(a)}$, $B^{(b)}$, and $B^{(c)}$ is well defined and finite. For convenience, we may first introduce a regulator of a heavy electron mass M, and make all regularized amplitudes $B^{(\mathrm{reg})(a,b,c)}$ finite. We finally let M go to infinity after we complete our calculation.

Since $B=B(p_+q_-;\mathbf{p},\mathbf{q})$, we can evaluate B for a fixed $p_+=1$ (or, alternatively, $q_-=1$).[21] It is actually more convenient to compute directly the coefficient of $s\ln s$, which is

$$J^{(a)}=\int_{-\infty}^{\infty}\frac{dq_-}{4\pi}B_{--,++}{}^{(a)}(p_+=1,q_-;\mathbf{p},\mathbf{q})$$
$$=-\int\frac{dq_-}{4\pi}\frac{dW_+dW_-d^2W}{2(2\pi)^4}N^{(a)}(D_1D_2D_3D_4)^{-1}. \quad (3.12)$$

In terms of the parametrization $W=(W_+,\mathbf{W},W_-)$, we have

$$\begin{aligned}D_1&=(W_+-1)W_--\mathbf{W}_1{}^2-m^2+i\epsilon,\\ D_2&=W_+W_--\mathbf{W}_2{}^2-m^2+i\epsilon,\\ D_3&=W_+(W_-+q_-)-\mathbf{W}_3{}^2-m^2+i\epsilon,\\ D_4&=(W_+-1)(W_-+q_-)-\mathbf{W}_4{}^2-m^2+i\epsilon.\end{aligned} \quad (3.13)$$

Hence, we can write

$$J^{(a)}=-\int\frac{dW_+d^2W}{2(2\pi)^3}N^{(a)}$$
$$\times\int\frac{dW_-}{2\pi}(D_1D_2)^{-1}\int\frac{dq_-}{4\pi}(D_3D_4)^{-1}. \quad (3.14)$$

The dW_- and dq_- [actually $d(q_-+W_-)$] integrals can be worked out independently. Both integrals vanish except for $0<W_+<1$. This will automatically set a finite limit of integration on W_+, and is a common feature of infinite-momentum calculations. For $0<W_+<1$, we have

$$\int dW_-(D_1D_2)^{-1}=\frac{2\pi i}{W_+(\mathbf{W}_1{}^2+m)+(1-W_+)(\mathbf{W}_2{}^2+m^2)},$$
$$\int d(q_-+W_-)(D_3D_4)^{-1}=\frac{2\pi i}{W_+(\mathbf{W}_4{}^2+m^2)+(1-W_+)(\mathbf{W}_3{}^2+m^2)}. \quad (3.15)$$

[21] The calculation given here is very similar to the Compton scattering calculation given in the second paper of Ref. 16.

Hence,

$$J^{(a)}=\int_0^1\frac{dW_+d^2W}{32\pi^3}N^{(a)}$$
$$\times\frac{1}{W_+(\mathbf{W}_1{}^2+m^2)+(1-W_+)(\mathbf{W}_2{}^2+m^2)}$$
$$\times\frac{1}{W_+(\mathbf{W}_4{}^2+m^2)+(1-W_+)(\mathbf{W}_3{}^2+m^2)}$$
$$=\int_0^1 d\alpha dx\frac{d^2W}{32\pi^3}N^{(a)}(x\beta\mathbf{W}_1{}^2+x\alpha\mathbf{W}_2{}^2$$
$$+y\alpha\mathbf{W}_3{}^2+y\beta\mathbf{W}_4{}^2+m^2)^{-2}, \quad (3.16)$$

where x, y $(x+y=1)$ are Feynman parameters, and

$$\alpha\equiv 1-W_+,\quad \beta\equiv W_+. \quad (3.17)$$

Note that there is a complete symmetry between $\mathbf{W}_{1,2}\rightarrow\mathbf{W}_{3,4}$. This implies that if we had evaluated $J^{(a)}$ by fixing $q_-=1$, and integrating over p_+, we would have gotten the identical answer.

The remaining W integrals can be done straightforwardly by first making a translation

$$\mathbf{W}\rightarrow\mathbf{W}'=x\beta\mathbf{W}_1+x\alpha\mathbf{W}_2+y\alpha\mathbf{W}_3+y\beta\mathbf{W}_4$$
$$=\mathbf{W}+x\beta\mathbf{p}_1+y\alpha\mathbf{q}_1+y\beta(\mathbf{q}_1-\mathbf{p}_2). \quad (3.18)$$

Then the denominator becomes

$$\mathbf{W}'^2+m^2+xy\mathbf{K}^2+\alpha\beta\mathbf{K}'^2+xy\alpha\beta\mathbf{k}^2, \quad (3.19)$$
$$\mathbf{K}\equiv\alpha\mathbf{q}_1-\beta\mathbf{q}_2,\quad \mathbf{K}'\equiv x\mathbf{p}_1-y\mathbf{p}_2. \quad (3.20)$$

The final expression for $J^{(a)}$ is

$$J^{(a)}(\mathbf{p},\mathbf{q})=-\frac{1}{3\pi^2}\mathbf{k}^2\ln M^2+\frac{1}{\pi^2}\int_0^1 dxd\alpha$$
$$\times\{-\ln(m^2+R)[(\Delta_1+\Delta_3)\cdot(\Delta_2+\Delta_4)-2R]$$
$$+[1/(m^2+R)][(\Delta_1\cdot\Delta_2-R)(\Delta_3\cdot\Delta_4-R)$$
$$+(\Delta_1\cdot\Delta_4-R)(\Delta_2\cdot\Delta_3-R)$$
$$-(\Delta_1\cdot\Delta_3-R)(\Delta_2\cdot\Delta_4-R)]\}, \quad (3.21)$$

where M^2 is a cutoff mass of electron regulator [the $1/(M^2+R)$ term $\rightarrow 0$ as $M\rightarrow\infty$] and

$$\begin{aligned}R&\equiv xy\mathbf{K}^2+\alpha\beta\mathbf{K}'^2+xy\alpha\beta\mathbf{k}^2,\\ \Delta_1&\equiv\mathbf{W}_1-\mathbf{W}'=-y\mathbf{K}+\alpha\mathbf{K}'+\alpha y\mathbf{k},\\ \Delta_2&\equiv\mathbf{W}_2-\mathbf{W}'=-y\mathbf{K}-\beta\mathbf{K}'-y\beta\mathbf{k},\\ \Delta_3&\equiv\mathbf{W}_3-\mathbf{W}'=x\mathbf{K}-\beta\mathbf{K}'+x\beta\mathbf{k},\\ \Delta_4&\equiv\mathbf{W}_4-\mathbf{W}'=x\mathbf{K}+\alpha\mathbf{K}'-x\alpha\mathbf{k}.\end{aligned} \quad (3.22)$$

The quadratically divergent part disappeared identically after we subtracted the regulator term. As we shall see, the remaining logarithmic divergence is canceled by a similar term appearing in Figs. 7(b) and 7(c). Thus the

final result does not depend on the regulator mass and is finite.

Let us consider the contributions from Figs. 7(b) and 7(c). The leading term is

$$B_{--,++}{}^{(b)}(p,q)=-\int\frac{d^4W}{(2\pi)^4}N^{(b)}(D_1D_2D_3D_4)^{-1}, \quad (3.23)$$

with

$$N^{(b)}=\mathrm{Tr}[(W_1+m)\gamma_-(W_2+m)\gamma_+ \times(W_3+m)\gamma_+(W_4+m)\gamma_-] =32W_+W_-(m^2+\mathbf{W}_2\cdot\mathbf{W}_4), \quad (3.24)$$

$$D_i=W_i{}^2-m^2+i\epsilon, \quad (3.25)$$

where W is the integration variable. It is chosen to be W_2. The W_i's, $i=1, 2, 3, 4$, are related to W through

$$W_1=W+p_1, \quad W_2=W, \quad W_3=W+q_1, \quad W_4=W+q_1+q_2=W+p_1+p_2.$$

The amplitude $B_{--,++}{}^{(c)}(p,q)$ can be obtained through the substitution $q_1\leftrightarrow q_2$ (or $p_1\leftrightarrow p_2$). In analogy to $J^{(a)}$, we have

$$J^{(b)}(\mathbf{p},\mathbf{q})=\int_{-\infty}^{\infty}\frac{dq_-}{4\pi}B_{--,++}{}^{(b)}(p_+=1,q_-;\mathbf{p},\mathbf{q}) \quad (3.26a)$$

$$=\int_{-\infty}^{\infty}\frac{dp_+}{4\pi}B_{--,++}{}^{(b)}(p_+,q_-=1;\mathbf{p},\mathbf{q}). \quad (3.26b)$$

Of course, Eqs. (3.26a) and (3.26b) should lead to the same result. We would like to point out that the only (q_1,q_2) dependence in $B_{--,++}{}^{(b),(c)}$ is through the denominator

$$D_3=(W+q_1)^2-m^2+i\epsilon=W_+(W_-+q_-) -(\mathbf{W}+\mathbf{q}_1)^2-m^2+i\epsilon. \quad (3.27)$$

After q_- integration, this $\mathbf{q}_1$ dependence in $J^{(b)}+J^{(c)}$ is washed out. Hence $J^{(b)}(\mathbf{p},\mathbf{q})+J^{(c)}(\mathbf{p},\mathbf{q})$ can depend only on the sum $\mathbf{q}_1+\mathbf{q}_2=\mathbf{k}$, but not on the individual $\mathbf{q}_i$. In other words, as one might expect, if two or more photons from the same side (here from the right-hand side) are inserted adjacent to each other onto an electron line of a bubble, the resultant amplitude depends only on the *sum* of their transverse momenta. We would like to point out that this result is not new, and has already appeared in the original ee, $e\gamma$, and $\gamma\gamma$ calculations.[6] We can apply this argument to the two-photon vertices on the left-hand side of the box diagram. Therefore, $J^{(b)}+J^{(c)}$ can only be a function of $\mathbf{k}$ $(=\mathbf{p}_1+\mathbf{p}_2=\mathbf{q}_1+\mathbf{q}_2)$. We have verified this $\mathbf{k}$ dependence for our box diagram explicitly by carrying out the parametric integrals below.

Once we know that $J^{(b)}+J^{(c)}$ depends only on $\mathbf{k}$, we can compute it easily by choosing $\mathbf{p}_1=\mathbf{q}_1=\mathbf{k}$, $\mathbf{p}_2=\mathbf{q}_2=0$. The result is

$$J^{(b)}+J^{(c)}=\int_{-\infty}^{\infty}\frac{dq_-}{4\pi}[B_{--,++}{}^{(b)}(p_+=1,q_-;\mathbf{p},\mathbf{q}) +B_{--,++}{}^{(c)}(p_+=1,q_-;\mathbf{p},\mathbf{q})] \quad (3.28)$$

$$=\int\frac{dW_+dW_-d^2W}{2(2\pi)^4}\frac{N^{(b)}}{D_1D_2D_4} \times\int_{-\infty}^{\infty}\frac{dq_-}{4\pi}\left(\frac{1}{D_3}+\frac{1}{D_3'}\right), \quad (3.29)$$

where $N^{(b)}=N^{(c)}=32W_+W_-(m^2+\mathbf{W}_2\cdot\mathbf{W}_4)$ and

$$D_3'=(W-q_1)^2-m^2+i\epsilon =W_+(W_--q_-)-(\mathbf{W}-\mathbf{q}_1)^2-m^2+i\epsilon.$$

The q_- integral is simple, and gives $-2\pi i/W_+$. Again $0\leq W_+\leq 1$. After performing the W_- integral we finally have

$$J^{(b)}+J^{(c)}=\frac{(-2\pi i)^2}{4\pi}\int\frac{dW_+d^2W}{2(2\pi)^4} \times32(\mathbf{W}_1{}^2+m^2)(\mathbf{W}_2\cdot\mathbf{W}_4+m^2) \times\frac{1}{W_+(\mathbf{W}_1{}^2+m^2)+(1-W_+)(\mathbf{W}_2{}^2+m^2)} \times\frac{1}{W_+(\mathbf{W}_1{}^2+m^2)+(1-W_+)(\mathbf{W}_4{}^2+m^2)}, \quad (3.30)$$

which is precisely $-J^{(a)}(\mathbf{p}_1=\mathbf{q}_1=k,\ \mathbf{p}_2=\mathbf{q}_2=0)$ in (3.16). Therefore, the total bubble contribution is

$$J(\mathbf{p},\mathbf{q})=J^{(a)}+J^{(b)}+J^{(c)} =\frac{1}{\pi^2}\int_0^1 dxd\alpha \times\{-\ln(m^2+R)[(\mathbf{\Delta}_1+\mathbf{\Delta}_3)\cdot(\mathbf{\Delta}_2+\mathbf{\Delta}_4)-2R] +[1/(m^2+R)][(\mathbf{\Delta}_1\cdot\mathbf{\Delta}_2-R)(\mathbf{\Delta}_3\cdot\mathbf{\Delta}_4-R) +(\mathbf{\Delta}_1\cdot\mathbf{\Delta}_4-R)(\mathbf{\Delta}_2\cdot\mathbf{\Delta}_3-R) -(\mathbf{\Delta}_1\cdot\mathbf{\Delta}_3-R)(\mathbf{\Delta}_2\cdot\mathbf{\Delta}_4-R)]\} -(\text{same expression with } \mathbf{p}_1=\mathbf{q}_1=\mathbf{k},\ \mathbf{p}_2=\mathbf{q}_2=0), \quad (3.31)$$

where the Δ_i's and R are given in (3.22). Equation (3.31) is manifestly finite and cutoff independent. The result obtained here is consistent with a recent calculation of Frolov *et al.*[12]

It is now straightforward to compute the contribution of the elastic amplitude $a+c\rightarrow a+c$ as in Fig. 3(a).

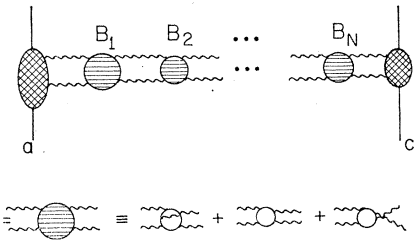

FIG. 8. Simple t-channel iteration of the simple two-photon → two-photon bubble $B_{2,2}$. We must consider all gauge possibilities within this picture.

Denote

$$I^{(a)}(\mathbf{p})\equiv\int[A_{++}(p_a';p_1',p_2')+A_{++}(p_a';p_2',p_1')]\frac{dp_+'}{4\pi},$$
$$I^{(c)}(\mathbf{q})\equiv\int[C_{--}(p_c'';q_1'',q_2'')+C_{--}(p_c'';q_2'',q_1'')]\frac{dq_-''}{4\pi}, \tag{3.32}$$

where $I^{(a)}$, $I^{(c)}$ in the simple case of two-photon exchange are the impact factors introduced by Cheng and Wu.[5] The contribution from various parts can be summarized as follows:

(1) There are factors $I^{(a)}(\mathbf{p})$ and $I^{(c)}(\mathbf{q})$ from the A_{++} and C_{--} integrals. The impact factor is defined as the integral of the sum of a diagram and its crossed diagrams. Hence, an over-all factor 1/2! should be included to correct the double counting in $I^{(a)}$ and $I^{(c)}$.

(2) There is a factor $(\ln s)/2\pi$ due to $\int dp_+/(4\pi p_+)$.

(3) For each exchanged photon (of momentum $\mathbf{p}$) between two electron lines, we include a factor $-ie^2/(\mathbf{p}^2+\mu^2)$. In the cases of e^-e^+, $e\gamma$, and $\gamma\gamma$ scattering, we encounter the exchange of photons between electron and positron. Then, a factor $ie^2/(\mathbf{p}^2+\mu^2)$ is included. Of course, the transverse momentum should be integrated over with volume $d^2p/(2\pi)^2$.

(4) There is an over-all factor $\frac{1}{4}s$.

Combining (1)–(4), we obtain the scattering amplitude for Fig. 3(a) as

$$M=\tfrac{1}{4}s\frac{\ln s}{4\pi}\int\int\frac{d^2p_1}{(2\pi)^2}\frac{d^2q_1}{(2\pi)^2}I^{(a)}(\mathbf{p})I^{(c)}(\mathbf{q})J(\mathbf{p},\mathbf{q})\times\frac{-ie^2}{\mathbf{p}_1^2+\mu^2}\frac{-ie^2}{\mathbf{p}_2^2+\mu^2}\frac{-ie^2}{\mathbf{q}_1^2+\mu^2}\frac{-ie^2}{\mathbf{q}_2^2+\mu^2}, \tag{3.33}$$

where $\mathbf{p}_1+\mathbf{p}_2=\mathbf{q}_1+\mathbf{q}_2=\mathbf{k}$.

We would like to mention briefly how repetition of these box diagrams can be computed in the present context. According to the analysis of kinematics developed in Sec. II, the amplitude for a multibox diagram (Fig. 8) can be factored into products of various pieces,

$$M^{(N)}=\frac{s}{2^{N+1}}\int A_{++}(p_a',q_1')\frac{dq_{1-}'}{4\pi}\times\prod_{n=1}^{N}\left[\int B_{--,++}{}^{(n)}(q_{(2n)}',q_{(2n+1)}')\times\frac{dq_{(2n)+}'}{4\pi}\frac{dq_{(2n+1)-}'}{4\pi}\int C_{--}(q_{(2N+2)}',p_c'')\frac{dq_{(2N+2)+}'}{4\pi}\right]\times\prod_{n=1}^{N+1}\left(\frac{ie^2}{\mathbf{q}_{(2n)1}{}^2+\mu^2}\frac{ie^2}{\mathbf{q}_{(2n)2}{}^2+\mu^2}\right)\frac{d^2q_{(n)}}{(2\pi)^2},$$

where q_{2n}, q_{2n+1} denote the momentum of photons attaching to the nth bubble in the frame appropriate to the description of that bubble, $\mathbf{q}_{2n+1}=\mathbf{q}_{2n}$. For the initial and final blobs, we have

$$I^{(a)}=\int[A_{++}(p_a';q_{(1)1}',q_{(1)2}')+A_{++}(p_a';q_{(1)2}',q_{(1)1}')]\frac{dq_{(1)}'}{4\pi},$$
$$I^{(c)}=\int[C_{--}(p_c'';q_{(2N+2)1}',q_{(2N+2)2}')+C_{--}(p_c'';q_{(2N+2)2}',q_{(2N+2)1}')]\frac{dq_{(2N+2)}'}{4\pi},$$

while for the nth bubble,

$$\int B_{--,++}{}^{(n)}(q_{(2n)+}'=1,q_{(2n+1)}')\frac{dq_{(2n+1)-}'}{4\pi}=J(\mathbf{q}_{(2n)},\mathbf{q}_{(2n+1)}).$$

The contribution from the phase-space integrals $\prod\int dq_{(2n)+}'/4\pi q_{(2n)+}'$ are rather straightforward. Each of the integrals leads to a factor $(\ln s)/2\pi$. (Recall that $q_{(2n)+}$ can be both positive and negative.) Since the integration variables are ordered $q_{2+}>q_{4+}>\cdots>q_{2N+}$, a factor $1/N!$ should be included as an over-all factor, giving

$$\frac{1}{N!}\left(\frac{\ln s}{2\pi}\right)^N.$$

Hence,

$$M^{(N)}=\frac{1}{N!}\frac{s}{4}\left(\frac{\ln s}{4\pi}\right)^N\int\cdots\int I^{(a)}(\mathbf{q}_{(1)})I^{(c)}(\mathbf{q}_{(2N+2)})\times\prod_{n=1}^{N}[J(\mathbf{q}_{(2n)},\mathbf{q}_{(2n+1)})]\times\prod_{n=1}^{N+1}\left(\frac{d^2q_{(2n)}}{(2\pi)^2}\frac{-ie^2}{\mathbf{q}_{(2n)1}{}^2+\mu^2}\frac{-ie^2}{\mathbf{q}_{(2n)2}{}^2+\mu^2}\right).$$

The sum over all N at $t=0$ of this result was obtained earlier in Ref. 12 by solving the Bethe-Salpeter equation. The $(\ln s)^N$ factor emerges naturally in our calcula-

tion as the multibubble phase-space factor. We shall discuss this point further in Sec. VI.

IV. FURTHER GENERAL RESULTS

In this section we would like to examine some other "primitive" diagrams of the same general type as is discussed in Sec. III. These diagrams are shown in Figs. 9(a)–9(c). We assume that we have accomplished the kind of factorization we discussed in Sec. II and that these diagrams represent "units" in some larger diagram associated with, say, elastic scattering of leptons. The cross-hatched blobs in these diagrams are "primitive" blobs, i.e., they cannot be cut in two by crossing photon lines only. As we mentioned in Sec. II, this means that the leading $\ln s$ behavior is fixed. The simplest example of such a primitive blob would be a simple lepton loop. Charge-conjugation invariance (i.e., Furry's theorem) tells us that the total number of photon lines connecting to a blob, primitive or otherwise, must be even. Finally, in diagrams 9(a)–9(c) we remember a left-hand photon line connects to the primitive blob with coupling γ_- and a right-hand photon line connects to the primitive blob with coupling γ_+.

We shall treat diagrams 9(a)–9(c) in what follows. Our conclusions are the following for the case where these diagrams connect directly to external fermions. Diagram 9(a) contributes to only $O(1)$ rather than $O(s\ln s)$; diagram 9(b) contributes to only $O(s)$ rather than $O(s\ln s)$; and diagram 9(c) contributes $O(s\ln s)$. In the general case when diagrams 9(a)–9(c) are subdiagrams of a larger diagram, we find that diagrams with 9(a) as a subdiagram do not contribute to the leading s behavior, those with 9(b) as a subdiagram do not contribute to the leading $s(\ln s)^N$ behavior, while those with 9(c) as a subdiagram contribute to the leading $s(\ln s)^N$ behavior, with $N=$number of primitive bubbles. In other words, when we inspect the leading $\ln s$ behavior, we only count the primitive diagrams of type 9(c).

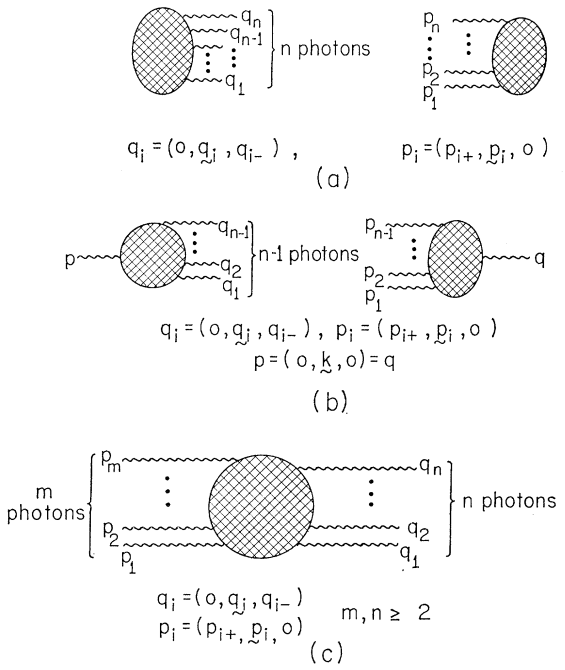

FIG. 9. Some more general primitive bubbles, with appropriate momentum labeling. (a) n photons attach to a bubble all from the same side; (b) all but one of n photons attach from the same side; (c) m photons attach from one side, n from the other, with m, $n\geq 2$. When $m=n=2$, we have $B_{2,2}$.

A. Diagram 9(a)

If this diagram were connected directly to one of the external lepton lines, it would look like a class of self-energy corrections to the lepton. Thus, at least in this case, one would feel unhappy if any s dependence at all were introduced by this diagram. In fact, s dependence is never introduced by this diagram. This is seen as follows. Consider the left-hand diagram of Fig. 9(a) for $n=4$, for definiteness (the argument generalizes in an obvious way). The diagram is then of the form

$$B_{\alpha\beta\gamma\delta}(q_1,q_2,q_3,q_4)\Rightarrow B_{++++}(q_1,q_2,q_3,q_4)\,, \qquad (4.1)$$

where

$$q_i=(0,\mathbf{q}_i,q_{i-})\,. \qquad (4.2)$$

Now, the question is whether one can construct a fourth-rank tensor with nonvanishing plus components. The answer is no by simple inspection: This tensor has to be constructed from q_i and the numerical tensors $g_{\mu\nu}$ and $\epsilon_{\mu\nu\lambda\sigma}$. Since q_i has no plus component [actually $q_{i+}=O(1/s)$] and $g_{++}=g_{+\perp}=0$, $g_{\mu\nu}$ and q_μ will not contribute any plus component. Similarly, one finds that $\epsilon_{\mu\nu\lambda\sigma}$ will not contribute either because the triple product vanishes,

$$\epsilon_{+\mu\nu\lambda}q_1^{\mu}q_2^{\nu}q_3^{\lambda}=\tfrac{1}{2}\epsilon_{+-lm}[(q_1)_+(q_2)_l(q_3)_m+\cdots]=0$$

(note that $\epsilon_{++\mu\nu}=0$). Thus B_{++++} is of $O(1/s)$ at least.

When this diagram is associated with the other factors which go to make up the scattering amplitude, this $1/s$ will cancel, leaving us with an amplitude of $O(1)$ rather than $O(s)$ or $O(s\ln s)$. More precisely, when this diagram is inserted anywhere in a "factorized" amplitude, it contributes no further s dependence.

B. Diagram 9(b)

If this diagram were connected directly to the two external lines in an elastic scattering process, it would look like a single exchanged photon with a vertex correction. Thus, at least in this case, one would feel unhappy if an s dependence beyond that of single-photon exchange [which is $O(s)$] were introduced by this diagram. In fact, we can show that $\ln s$ terms are never introduced by this diagram no matter where it is inserted in a "factorized" amplitude.

For definiteness, consider the left-hand diagram of Fig. 9(b) in the case $n-1=3$ (again, the argument is

easily generalized for $n-1$ any odd number >1). The diagram is of the form

$$B_{-+++}(p;q_1,q_2,q_3), \tag{4.3}$$

where q_i is given by Eq. (4.2), and where

$$p=(0,\mathbf{k},0). \tag{4.4}$$

p has no plus component for the usual reason that left-hand photons have no plus component, namely, to conserve the total plus component across the diagram. It also has no minus component, because it is connected from the left-hand side of the bubble. We can now make a tensor argument of the same type as the one we made in Sec. IV A. All the momentum vectors upon which this tensor could depend have zero plus component. We could think of forming B_{-+++} with vectors of the type $g_{\mu\nu}q_{1\lambda}q_{2\sigma}$ or $\epsilon_{\mu\nu\alpha\beta}q_{1\alpha}q_{2\beta}$, etc. Even though g_{-+} and $\epsilon_{-+\alpha\beta}$ are nonzero, g_{++} and $\epsilon_{++\alpha\beta}$ are zero. Thus, we can only take care of one pair of indices $(-+)$; the remaining indices $++$ can never be constructed.

Thus this diagram is by itself $O(1/s)$. Unlike diagram 9(a), however, this diagram connects on *both* sides to factorized pieces. This factorization automatically contributes $O(s)$ on either side, so when integrated into a complete scattering amplitude, diagram 9(b) gives $O(s)$, but not $O(s\ln s)$.

C. Diagram 9(c)

None of the agruments of Secs. IV A and IV B applies to this particular diagram to rule out logarithmic factors. Instead, we can use the techniques of Sec. III to study this case and to conclude that it contributes $O(s\ln s)$ when connected directly to external lepton lines. This diagram is of the form

$$B_{m,n}(p_{1+},\ldots,p_{m+};q_{1-},\ldots,q_{n-};\ \text{transverse momenta}), \tag{4.5}$$

where the subscripts m, n denote that B has m minus indices and n plus indices. Under a boost along the z direction,

$$p_+\to p_+'=e^{\lambda}p_+,\quad q_-\to q_-'=e^{-\lambda}q_-,\quad \mathbf{p}'=\mathbf{p},\quad \mathbf{q}'=\mathbf{q}, \tag{4.6}$$

we have

$$B_{m,n}(e^{\lambda}p_{i+},e^{-\lambda}q_{j-};\ \text{transverse quantities}) = e^{\lambda(n-m)}B_{m,n}(p_{i+},q_{j-};\ \text{transverse quantities}). \tag{4.7}$$

Equation (4.7) implies that the expression

$$\prod_{i=1}^{m}dp_{i+}\prod_{j=1}^{n}dq_{j-}\times B_{m,n}(p_{i+},q_{j-};\ \text{transverse quantities}) = \prod_{i=1}^{m}dp_{i+}'\prod_{j=1}^{n}dq_{j-}'\times B_{m,n}(p_{i+}',q_{j-}';\ \text{transverse quantities}) \tag{4.8}$$

is invariant under a "p-independent" boost.

Let us boost so that any one of the p_i variables has plus component equal to 1, or any one of the q_i variables has minus component equal to 1. In general, a single boost gives this for only a single variable. For example, boost in the three-direction so that $p_{1+}'=1$. This boost is parametrized by "rapidity" λ,

$$p_{1+}'=e^{\lambda}p_{1+}=1. \tag{4.9}$$

Then

$$p_{i+}'=p_{i+}/p_{1+}\quad(i=2,3,\ldots,m),\qquad q_{j-}'=q_{j-}p_{1+}\quad(j=1,2,\ldots,n) \tag{4.10}$$

are a new set of $m+n-1$ variables on which Eq. (4.5) depends. The transverse quantities are of course not affected by this boost. In this new frame, the multiple integral of (4.8) over dp_{i+} and dq_{i-} becomes

$$\int\prod_{i=1}^{m}\prod_{j=1}^{n}dp_{i+}dq_{j-}\times B_{m,n}(p_{i+};q_{j-};\ \text{transverse quantities}) = \int\frac{dp_{1+}}{p_{1+}}\int\prod_{i=2}^{m}\prod_{j=1}^{n}dp_{i+}'dq_{j-}'\times B_{m,n}(1,p_{i+}';q_{j-}';\ \text{transverse quantities}), \tag{4.11}$$

where dp_{i+}' in (4.8) is replaced by dp_{1+}/p_{1+}, and the remaining integral is p_{1+} independent. For convenience, we have left two δ functions out of Eq. (4.11), one conserving the total plus momentum for the p variables and one conserving the total minus momentum for the q variables. Thus, instead of depending on $m+n-1$ ratios (variables), B actually depends on $m+n-3$ variables. In the special case of $m=n=2$ which was worked out in Sec. III, the amplitude depends on $2+2-3=1$ remaining value.

Connecting diagram 9(c) directly to the external lines introduces, in addition to the extra $\ln s$ factor from $\int dp_{1+}/p_{1+}$, a single power of s. Thus the primitive bubble of diagram 9(c) gives, for elastic scattering of leptons, $O(s\ln s)$. In the general case of the insertion of diagram 9(c) into a larger graph, we always find an extra $\ln s$ factor. This additional $\ln s$ factor comes from the longitudinal phase-space integral $\int dp_{1+}/p_{1+}$. Of course, the contribution of this bubble does not depend on which of the particular reference momenta $p_{i+}'=1$ (or $q_{j-}'=1$) we choose.

The conclusion of this section is that for the contribution of primitive blobs to elastic scattering, only diagram 9(c) gives as much as $s\ln s$. Since the $m=n=2$ minimizes the power of α, the diagram studied in Sec. III gives the leading behavior in $\ln s$ for this entire class of diagrams.

V. s-CHANNEL ITERATION

We have made careful distinction between primitive and nonprimitive bubbles in the preceding sections.

This distinction is necessary in order to understand the behavior of a particular diagram in $\ln s$ as $s \to \infty$; its formulation is necessary in order to understand the t-channel iteration of bubbles or to the establishment of a Bethe-Salpeter equation that sums these t-channel iterations.

In this section we would like to discuss briefly the corresponding distinction which is necessary in order to understand s-channel iteration. We must therefore define "connected" and "disconnected" diagrams. Suppose that we have now accomplished the factorization of a given diagram into three parts, one depending on each of the two external leptons, and one depending on all possible multiphoton interactions in the middle. Concentrate now only on this middle part. If this middle part falls into two or more distinct pieces (without cutting any lines), then we say it is *disconnected*. If, on the other hand, it does not do so, it is a *connected* diagram. Simple examples of these two diagrams are shown in Figs. 10(a) and 10(b).

We can call a connected diagram a connected *unit*, and imagine forming a disconnected diagram by the exchange of two or more of these connected units. Such a diagram is shown in Fig. 10(a) for the exchange of two of the connected units studied in Sec. III. We say we have nth-order exchange of a given unit when n units are exchanged and we sum these diagrams with the photon lines of each unit attached to the external line parts in all possible ways. The s dependence of an nth-order exchange in which m primitive bubbles appear over-all is just $s(\ln s)^m$. As we shall discuss below, the t dependences of iterations of a given unit is different but closely related.

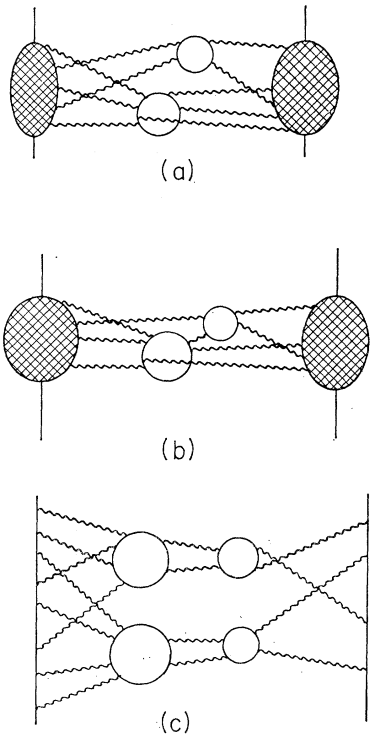

FIG. 10. Disconnected and connected diagrams. (a) Simple example of a disconnected diagram; (b) simple example of a connected diagram; (c) typical disconnected diagram which is the exchange of two identical connected units.

Let us consider the amplitude for a process containing n identical connected units as shown in Fig. 10(c). Actually, we can include all kinds of radiative corrections to the incident particles as long as we ignore the contribution due to fermion pairs.[22] In that case, the t dependence of an nth-order exchange diagram is as follows. Let exchange of a single unit have t (and s) dependence $F(s,t)$, and let the Fourier transform of $F(s,t)$ over k be given by

$$-i\chi(s,\mathbf{b}) = \int e^{i\mathbf{k}\cdot\mathbf{b}} F(s,\mathbf{k}^2) d^2k \frac{1}{(2\pi)^2}. \tag{5.1}$$

The s dependence in $F(s,t)$ is simply a multiplicative factor $(\ln s)^N$, with N being the number of primitive bubbles in the unit. The same $\ln s$ dependence also appears in $\chi(s,\mathbf{b})$. Then the nth-order exchange diagram has t dependence with Fourier transform (see the Appendix)

$$(1/n!)[-i\chi(s,\mathbf{b})]^n. \tag{5.2}$$

This is the well-known eikonal property. In particular, the sum over n of all nth-order exchanges is

$$\exp[-i\chi(s,\mathbf{b})]-1. \tag{5.3}$$

Actually, when more than one connected piece are iterated, the eikonal form persists. The over-all χ is the sum of individual χ's, as demonstrated in the Appendix. This exponentiation property has been shown explicitly by several authors[6,7] when the unit is single-photon exchange. For the unit studied in Sec. III,[23] one has explicitly

$$\begin{aligned} F(s,t) = \frac{\ln s}{4\pi} \int \prod_{ij} \frac{d^2p_i}{(2\pi)^2} \frac{d^2q_j}{(2\pi)^2} \\ \times J(\mathbf{p},\mathbf{q}) \prod_{i,j=1}^{2} \frac{-ie^2}{\mathbf{p}_i^2+\mu^2} \frac{-ie^2}{\mathbf{q}_j^2+\mu^2} \\ \times (2\pi)^2\delta(\mathbf{p}_1+\mathbf{p}_2-\mathbf{k})(2\pi)^2\delta(\mathbf{q}_1+\mathbf{q}_2-\mathbf{k}), \end{aligned} \tag{5.4}$$

where $J(\mathbf{p},\mathbf{q})$ is given in Eq. (3.31). The Fourier transform of $F(s,t)$ is

$$-i\chi(s,\mathbf{b}) = \ln s\, \alpha(\mathbf{b}), \tag{5.5}$$

[22] S. J. Chang, Phys. Rev. D **1**, 2977 (1970); Y. P. Yao, *ibid.* **1**, 2971 (1970).

[23] The possibility that the s-channel iterations of an arbitrary connected piece should exponentiate was pointed out to one of us (S.J.C.) some time ago by Professor S. Adler, to whom we are indebted. See H. Cheng and T. T. Wu, Phys. Rev. **186**, 1611 (1969). These authors also showed that $B_{2,2}$ exponentiates after s-channel interactions.

where

$$\alpha(\mathbf{b})=\frac{1}{4\pi}\int\frac{d^2k}{(2\pi)^2}e^{i\mathbf{k}\cdot\mathbf{b}}\times J(\mathbf{p},\mathbf{q})\prod_{ij}\frac{d^2p_i}{(2\pi)^2}\frac{d^2q_j}{(2\pi)^2}\frac{-ie^2}{\mathbf{p}_i^2+\mu^2}\frac{-ie^2}{\mathbf{q}_j^2+\mu^2}\times(2\pi)^2\delta(\mathbf{p}_1+\mathbf{p}_2-\mathbf{k})(2\pi)^2\delta(\mathbf{q}_1+\mathbf{q}_2-\mathbf{k}). \quad (5.6)$$

Hence, the resultant amplitudes behave like

$$\tfrac{1}{2}s\delta_{aa'}\delta_{cc'}m^{-2}\int d^2b\,e^{-i\mathbf{k}\cdot\mathbf{b}}\{\exp[-i\chi(s,\mathbf{b})]-1\}=\tfrac{1}{2}s\delta_{aa'}\delta_{cc'}m^{-2}\int d^2b\,e^{-i\mathbf{k}\cdot\mathbf{b}}(s^{\alpha(b)}-1), \quad (5.7)$$

where $\delta_{aa'}$ and $\delta_{bb'}$ imply that the helicities of the initial and final electrons do not change. Equation (5.7) helps exhibit the j-plane cut structure of the amplitude for multiple exchange. We would like to point out that Eq. (5.7) applies to the s-channel iteration of *all* connected diagrams involving only *one* primitive bubble, such as in Fig. 9(c). In this case the amplitude of the connected piece has a $(\ln s)^1$ dependence, $F(s,t)=\ln s\, f(t)$. Hence, $-i\chi(s,b)=\ln s\,\alpha'(b)$, as in (5.5) and (5.7). Of course, the $\ln s$ dependence will be different if the connected piece contains N primitive bubbles for $N>1$ [e.g., in Fig. 10(c), the connected piece contains two primitive bubbles]. In the latter case, $F(s,t)=(\ln s)^N f(t)$ and, consequently,

$$-i\chi(s,b)=(\ln s)^N\alpha''(b).$$

Then, the s dependence in the s-channel iterated amplitude,

$$s\int d^2b\,e^{-i\mathbf{k}\cdot\mathbf{b}}[e^{-i\chi(s,b)}-1],$$

is completely different, and we encounter a j-plane structure which is richer than that supplied by simple s-channel iterated primitive unit exchange, given by (5.7). At present we cannot say as much as we would like to about the exact behavior of the full amplitude, which is generated by the sum of all possible connected pieces. Questions about the complete j-plane structure, the nature of the branch points, discontinuities, cancellation of the Gribov-Pomeranchuk singularity, etc., are all left open. Further explorations along this line are certainly desirable. What little we can say is outlined in Sec. VII.

VI. INELASTIC PROCESSES

We shall discuss briefly the factorization properties of an inelastic production process. For simplicity, let us first analyze the production process without the center bubble [Fig. 11(a)]. The invariant amplitude for the process of Fig. 11(a) is

$$\mathfrak{M}=\int A_{\alpha\beta\ldots\gamma}(p_a,q)C_{\alpha\beta\ldots\gamma}(p_c,q)\times\prod_j\frac{ie^2}{q_j^2-\mu^2+i\epsilon}\frac{d^4q_j}{(2\pi)^4}(2\pi)^4\delta^4(\textstyle\sum q_j-k), \quad (6.1)$$

where $p_a=\{p_a,p_{aj}\}$ stands for initial and product particle momenta due to particle a, p_c for particle c, where the q's are the momenta of the exchanged photons, and where k^μ is the total momentum transferred, all in the c.m. frame. For simplicity, we choose the three-momentum $\mathbf{p}_a=(0,0,P)=-\mathbf{p}_c$, $P\approx\sqrt{s}$. We are interested in reactions in which the momentum transfer k^μ is finite. Unlike the elastic process, the final particle numbers and the effective mass of each of the two jets of particles may not remain finite. However, we shall study the case of a finite number of final particles with a finite total mass. This restriction turns out to be rather important in what follows. In particular, the leading s behavior of the invariant amplitude can be explicitly factored, in a manner similar to that of Sec. II. Since the method is identical to the one used for the elastic amplitude, we shall not repeated the reduction here. The amplitude for large s reduces to

$$\mathfrak{M}=\tfrac{1}{2}s\int A_{++\ldots+}(p_a',q')\times\prod_j\frac{dq_{j-}'}{4\pi}4\pi\delta(\textstyle\sum q_{j-}'+p_a'-\sum p_{ai-}')C_{--\ldots-}(p_c'',q'')\times\prod_j\frac{dq_{j+}''}{4\pi}4\pi\delta(\textstyle\sum q_{j+}''+\sum p_{ci+}''-p_{c+}'')\times\prod_{(\text{all photons})}\frac{-ie^2}{\mathbf{q}^2+\mu^2}\frac{d^2q}{(2\pi)^2}(2\pi)^2\delta^{(2)}(\textstyle\sum\mathbf{q}-\mathbf{k}), \quad (6.2)$$

which is similar in form to Eqs. (2.12) and (2.17). However, note that $A_{++\ldots+}(p_a',q')$, for example, depends not only on the incident and exchange photon momenta in the standard frame a,

$$p_{a+}'=p_{a+}/\sqrt{s}=1,\quad \mathbf{p}_a'=0,\quad p_{a-}'=m^2,\quad q_{i+}'=0,\quad \mathbf{q}_i'=\mathbf{q}_i,\quad q_{i-}'=\text{finite} \quad (6.3)$$

but also on the final-particle momenta in the same standard frame:

$$p_{aj+}'\equiv x_j=p_{aj+}/\sqrt{s},\quad \mathbf{p}_{aj}'=\mathbf{p}_{aj},\quad p_{aj-}'=(\mathbf{p}_{aj}^2+m_{aj}^2)/x_j, \quad (6.4)$$

where x_i is the fraction of the longitudinal momentum taken by particle a_i, etc. As $s\to\infty$, the final states we are interested in are those with p_{ai}' approaching a finite limit. Physically, it is plausible that the final-state momenta might approach finite limits as $s\to\infty$ in the standard frame. It follows from the fact that in the

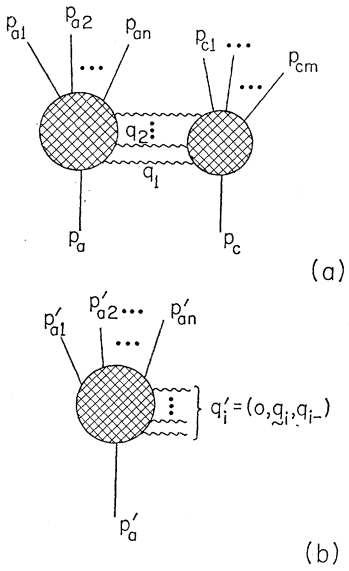

FIG. 11. (a) Inelastic diagram with multiphoton exchange and no bubbles in the middle. This diagram factors as does the elastic one. (b) The left-hand blob in its standard frame. In this frame, the q_{j+}' are zero.

standard frame, the momenta of the incident particle a and exchange photons all tend to a finite limit, as $s\to\infty$. We are effectively studying the scattering of particle a by multiphotons, all with finite momenta [see Fig. 11(b)]. Hence, the final particles produced should have finite momenta.

Similarly, we find that $C_{--\cdots-}(p_c'',q'')$ depends on the final quantities p_c'', p_{cj}'', and q'', which are finite in standard frame c. Hence, in analogy to the elastic scattering, the amplitude factors into two parts as $s\to\infty$. These parts are separately finite and may have limiting distributions. The significance of this result and its relation to the theory of limiting fragmentation[3] are discussed in Sec. VII.

The differential cross section for the production process Fig. 11(a) is

$$d\sigma=|\mathfrak{M}|^2\frac{1}{|v_a-v_c|}\frac{1}{2E_a}\frac{1}{2E_c}(\text{P.S.F.})$$

$$=|\mathfrak{M}|^2\frac{1}{2s}(\text{P.S.F.}), \tag{6.5}$$

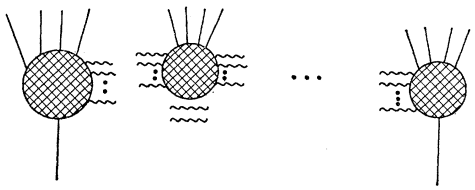

FIG. 12. Inelastic diagram with bubbles. The bubbles can contribute to the inelasticity by "evaporating" particles in the bubble's rest frame.

where the phase-space factor (P.S.F.) at $s\to\infty$ is

$$\text{P.S.F.}=(2\pi)^4\delta^4\Big(\sum p_{ai}+\sum p_{cj}-p_a-p_c\Big)\times\prod_i\delta(p_{ai}^2-m_{ai}^2)\frac{d^4p_{ai}}{(2\pi)^3}\times\prod_j\delta(p_{cj}^2-m_{cj}^2)\frac{d^4p_{cj}}{(2\pi)^3}$$

$$=\frac{8\pi^2}{s}\delta\Big(\sum x_i-1\Big)\delta\Big(\sum y_j-1\Big)\times(2\pi)^2\delta\Big(\sum \mathbf{p}_{ai}+\sum \mathbf{p}_{cj}\Big)\times\prod_i\left(\frac{dx_i}{4\pi x_i}\frac{d^2p_{ai}}{(2\pi)^2}\right)\prod_j\left(\frac{dy_j}{4\pi y_j}\frac{d^2p_{cj}}{(2\pi)^2}\right), \tag{6.6}$$

with

$$y_j=p_{cj-}''.$$

Hence,

$$d\sigma=|(1/s)\mathfrak{M}|^2(2\pi)^2\delta\Big(\sum x_i-1\Big)\delta\Big(\sum y_j-1\Big)\times(2\pi)^2\delta\Big(\sum_i \mathbf{p}_{ai}+\sum_j \mathbf{p}_{cj}\Big)\times\prod_i\left(\frac{dx_i}{4\pi x_i}\frac{d^2p_{ai}}{(2\pi)^2}\right)\prod_j\left(\frac{dy_j}{4\pi y_j}\frac{d^2p_{cj}}{(2\pi)^2}\right). \tag{6.7}$$

The differential cross section indeed approaches a finite limit as $s\to\infty$.

Now, we consider a general scattering amplitude, Fig. 12, in which the middle bubbles emit some external particles. At present we assume that the number and the total mass of the emitted particles are finite.[24] Under these assumptions, we find that the factorization of the amplitude, in analogy to the derivation given in Sec. II, can be carried through. Hence, the final amplitude can be written as s multiplied by factors which are separately finite as $s\to\infty$. [For N bubbles without photon emission, we still have the $(\ln s)^N$ dependence in the amplitude as for the elastic case. When photons are emitted from the bubbles, $\ln s$ terms do not arise until we integrate over the final-particle phase space, i.e., in the cross section.]

Each of the factors correspond to a particular bubble (or target) with all particles emitted. These bubbles are linked together by internal photon lines. The contribution of any bubble is still translationally invariant in the $\ln p_+$ space (or, equivalently, it is invariant under a boost along the z direction) if we translate the bubble with all particles it emits *simultaneously*. This invariance property implies that the contribution to the differen-

[24] Actually, these two assumptions are related. A finite "total mass" of the emission particles certainly implies a finite number of emitted particles. Conversely, some lower-order calculations suggest that the inverse is also true, i.e., for a fixed number of emitted particles, the contribution due to a large total mass is damped in the amplitude. See also the remarks following Eq. (6.1).

tial cross section due to this *group* of emitted particles is invariant under a boost along the z direction. Hence, we find that the group of particles which are emitted from a given bubble are kinematically related and have finite momenta (as $s\to\infty$) in the rest frame of the bubbles. Two groups of particles that belong to two different bubbles are decoupled due to the factorization property. (This is certainly true for the longitudinal momentum distribution. For the transverse momentum, however, one has to conserve the over-all momentum carried by all these individual groups. Consequently, certain correlations are introduced.)

We therefore see that each group of particles behaves like a "fireball." We have to point out that this kind of fireball does *not* have a spherical distribution in its own c.m. frame in general. The fireball "remembers" the longitudinal direction of the collision in which it is produced. It has only a finite extension in the $\mathbf{p}$ and $\ln p_+$ space, and therefore may have an average distribution like a spheroid in the above momentum space. The consequences and possible relevance to strong interactions of this picture will be discussed in the next section.

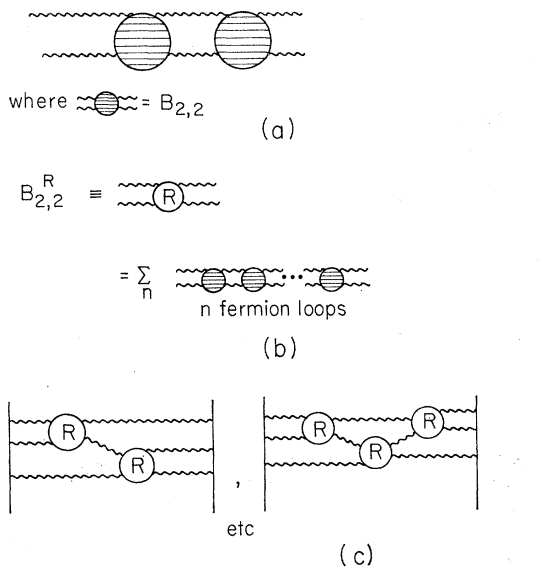

FIG. 13. t-channel iteration of the simple two-photon → two-photon bubble. (a) Double bubble; (b) $B_{2,2}{}^R$ is the sum of all t-channel iterations of $B_{2,2}$; (c) more general connected diagrams formed from $B_{2,2}{}^R$.

VII. DISCUSSION

We have seen in Sec. II that the properly renormalized gauge-invariant, two-photon bubbles (called $B_{2,2}$ here) give $\sim s\ln s\, f(t)$ when exchanged at high energies, as shown in Fig. 8. Furthermore, this is the leading connected primitive diagram as $s\to\infty$ and for small coupling α. As we have discussed in Sec. V, the fact that this is a connected diagram is significant for understanding the behavior in t. In this section we want to concentrate on behavior in s. As we have stated in Sec. II, it is the primitiveness or nonprimitiveness which helps to determine the behavior in $\ln s$.

In particular, consider the nonprimitive iteration of $B_{2,2}$, shown in Fig. 13(a) in second order. All possible permutations of photon lines are understood, in that figure, for gauge invariance. We have seen how invariance of this unit under three-direction boosts leads naturally to an s behavior

$$sf_2(t)(\ln s)^2.$$

$f_2(t)$ here depends, in particular, on the coupling. We can now treat the problem as a recursion problem by writing an nth-order iteration of $B_{2,2}$ as $B_{2,2}$ times an $(n-1)$th-order iteration. Either this approach or direct study of the nth-order iteration by invariance under boosts shows that this nonprimitive diagram behaves like $sf_n(t)\ (\ln s)^n$. One might hope that summation over all iterations of $B_{2,2}$ would lead to a simple behavior in s and $\ln s$. (The assumption here is as usual that summing the leading behavior gives the leading behavior of the sum.) This problem is a very well-known one, and a great deal of experience has been accumulated in the last several years,[25] especially on studies of $\lambda\phi^3$ theory. Studies of asymptotic behavior by means of the study of j-plane singularities has been of particular interest.[10]

Frolov *et al.*[12] in a recent Letter have accomplished this summation by using $B_{2,2}$ as the kernel in a Bethe-Salpeter equation. They solved the Bethe-Salpeter equation in the special case that the electron mass is zero and $t=0$. In this case they were able to find the leading j-plane singularities analytically. Their result has a branch point at $j=1+(11/32)\pi\alpha^2$. This behavior violates the Froissart bound, which states that the total cross section must not grow as fast as $s(\ln s)^2$. If we denote the sum of nth-order iterations of $B_{2,2}$ by $B_{2,2}{}^R$, as in Fig. 13(b), we can therefore conclude that the description of elastic scattering processes with $B_{2,2}{}^R$ alone is not satisfactory. Since iteration of $B_{2,2}$ generates the leading $(\ln s)^N$ amplitude for any fixed power in α (here α^{2N}), we must therefore include more complicated nonprimitive diagrams. Once we found a complete solution for $B_{2,2}{}^R$ (i.e., a solution for all momentum transfers), we could form more complicated nonprimitive diagrams using $B_{2,2}{}^R$ as a building block. Examples of such diagrams are shown in Fig. 13(c). We hope to study these problems more closely in the future. In Ref. 12, it was also suggested that the breakdown of the Froissart bound is due to the fact that the s-channel unitarity was not taken into account. How a satisfactory amplitude can be constructed is still an open question.

[25] See R. J. Eden *et al.*, *The Analytic S-Matrix* (Cambridge U. P., London, 1966).

It is worth noting here that in formulating s-channel elastic unitarity for the e-e scattering process, $B_{2,2}{}^R$ represents the contribution of multiperipheral-type processes to the intermediate states. This can be easily seen by cutting, for example, Fig. 2 horizontally. Thus the multiperipheral diagrams contribute the leading j-plane singularity at $t=0$. At least in QED we conclude that multiperipheral diagrams alone are inadequate for the saturation of elastic unitarity.

Among other general features of our calculations which may be relevant and applicable to hadron physics, we would like to mention again the factorization of the scattering amplitude into s-independent partial amplitudes. This factorization property generalizes to inelastic scattering as well. As shown in Sec. VI, the amplitudes of Fig. 11(a) in the limit of large s and finite t approach

$$M=\tfrac{1}{2}s\int A_{+\cdots+}(p_a',q')$$
$$\times\prod_j \frac{dq_{j-}'}{4\pi}4\pi\delta(\sum q_{j-}'+p_{a-}'-\sum p_{ai-}')$$
$$\times C_{--\cdots-}(p_c'',q'')$$
$$\times\prod_j \frac{dq_{j+}''}{4\pi}4\pi\delta(\sum q_{j+}''+\sum p_{ci+}''-p_{c+}'')$$
$$\times\prod_{\text{(all photons)}}\frac{-ie^2}{\mathbf{q}^2+\mu^2}\frac{d^2q}{(2\pi)^2}(2\pi)^2\delta^{(2)}(\sum\mathbf{q}-\mathbf{k}) \quad (6.2)$$

for fixed number of particles in the final states. As $s\to\infty$, both factors A and C approach a finite limit and become kinematically decoupled if the momenta of two groups of final particles are measured in their respective standard frames. This property is closely related to the idea of limiting fragmentation.[3] The standard frames for particles a and c are just the lab and projectile systems used by these authors.

The analogy between this calculation and Chou-Yang droplet-model-type result[1] does not end here. As Chang and Yao[22] have shown earlier, the contribution to the amplitude of the elastic blobs in Fig. 1(b) are proportional to the electromagnetic form factor squared if one suppresses the production of Fermion pairs in the vertex correction. This is also the lowest-order prediction of the droplet model. Recently, Lee[26] demonstrated that an operator droplet model can reproduce the field-theoretic results of Cheng and Wu[5] as to impact factors. The validity of this operator droplet model is based on the existence of certain limiting expressions. We conjecture that these restrictions are the same ones that ensure the validity of the factorization of the amplitude in Fig. 1(b).

The inclusion of bubbles in the middle together with the evaporation of photons and electron-positron pairs from the bubble (or pions and nucleon pairs in hadron physics) would represent a difference between our results and the presently formulated operator droplet model. These evaporation photons (or pions) may describe the pionization effect observed in cosmic-ray and high-energy data.[14] The detailed spectra and differential cross sections for these evaporation photons (or pions) are very model dependent, and probably do not have significant extrapolation to hadron physics. However, the following features seem to be quite general, and should be applicable to high-energy hadron scattering.[27,28]

(1) The bubble in the middle is invariant under translation in the $\ln p_+$ space. (Diagrammatically speaking, the plus component increases from right to left. This invariance is expressed by the freedom to "slide" the bubble horizontally.) Hence, the "pions" evaporated with low momentum relative to the bubble should have the analogous dp_+/p_+ distribution. In other words, these "pionization" products should have a flat distribution in a $\ln p_+$ plot (or, equivalently, in a $\ln p_-$ plot). The same kind of distribution was predicted by Feynman,[29] using some general physical arguments.

(2) The number of "pions" in a pionization process increases linearly with $\ln s$. This is essentially a pure volume effect in $\ln p_+$ space. More precisely, the average number of bubbles existing should be proportional to the available longitudinal phase space $\sim\ln s$, as should the total number of pions they evaporate. The above result is probably independent of the detailed structure of the bubbles and the fireballs they emitted, and depends only on the effect that the individual bubble and the particles it emitted are translationally invariant in the $\ln p_+$ space. The vectorial property of the exchanged photons plays a crucial role in the factorization property of the amplitude as well as in the translational invariance of the bubbles. Hence, one may expect the above conclusion not to be affected if one replaces the exchange (massive) photon in our model by any vector meson (e.g., ω meson), or by a flat Pomeranchon.

As a remark addressed to experimentalists, we would like to point out that the fireballs in our model may overlap because of independent translational freedom in the $\ln p_+$ space.

[26] B. Lee, Phys. Rev. D 1, 2361 (1970).

[27] These features are partially the result of the special limit $s\to\infty$, t small. Our previous experience (see Ref. 28) in the limit $s\to\infty$, $t\to\infty$, $s/t\to\infty$ indicates that the results described in this paper may not hold in this limit.

[28] S. J. Chang and P. M. Fishbane, Phys. Rev. Letters **24**, 847 (1970); preceding paper, Phys. Rev. D **2**, 1084 (1970).

[29] R. P. Feynman, Phys. Rev. Letters **23**, 1415 (1969).

(3) In analogy to the process of limiting fragmentation, it is conceivable from our model calculation that in the c.m. frame of any particular fireball, the distribution of n final particles in a fireball approaches a limit as $s \to \infty$.

(4) It is known that the average multiplicity in the high-energy collision $a+c \to$ (anything) increases at least as fast as $\ln s$ as $s \to \infty$. One or more of the following mechanisms may be responsible for this increase: (a) The total mass and the total number of the final particles in the target fragments may increase slowly as $s \to \infty$. This possibility is suggested by Yang,[30] and is conjectured by him as the dominant contribution to the increase of multiplicity. (b) According to our model, the multiplicity of fireballs increases as fast as $\ln s$. Then, the number of particles in the pionization will be proportional to $\ln s$, even though the average number of particles in a fireball is constant. As we mentioned earlier, this is a phase-space volume factor. There are several cosmic-ray experiments which support the existence and the rate of increase of the fireballs.[14] (c) In analogy to (a), the average multiplicity and the mass of the fireball may also increase slowly as $s \to \infty$. The total increase of multiplicity is determined by the combined effect of (a)–(c).

At present it is not clear which of these mechanisms is the dominant one. Future experiments and a more thorough model calculation may help us to distinguish various possibilities.

Note added in manuscript. During the typing of this paper there appeared in Phys. Rev. Letters **24**, 759 (1970), an interesting article by H. Cheng and T. T. Wu. These authors showed that the fixed branch point at $J=1$ for $t<0$ that is given by pure multiphoton exchange is modified when t is positive. In particular, for t at the elastic threshold, the amplitude behaves like $s^{3/2}$. They suggest that this is due to a moving pole emerging from the second sheet, and is another possible explanation for resolving Gribov's paradox.

ACKNOWLEDGMENT

The authors wish to thank Professor Lorella M. Jones for a critical reading of the manuscript.

APPENDIX

In this appendix, we wish to establish the general eikonalization for s-channel iteration of a connected piece. For definiteness, we consider the connected unit given in Fig. 14(a). As discussed in Sec. II, we only need to consider the diagram with plus components on particle a and minus components on particle c. The dominant amplitude at large s and fixed t, according to

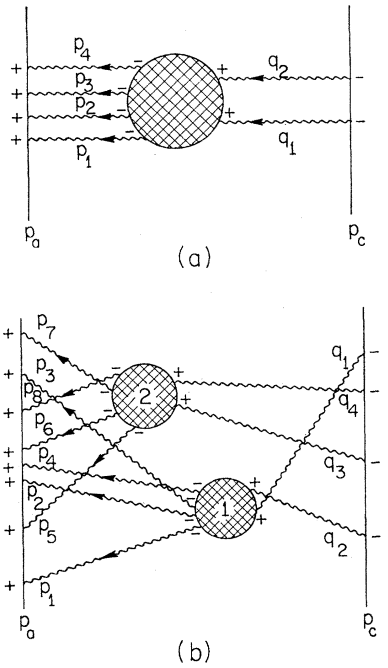

FIG. 14. s-channel iteration of a typical connected piece. (a) Bubble with four photons attaching from the left and two photons attaching from the right; (b) second-order iteration of diagram (a).

Eq. (2.17), is

$$M^{(1)}=\tfrac{1}{4}s\int A_4(p_a',p_i')\prod_i \frac{dp_{i-}'}{4\pi}4\pi\delta(\sum p_{i-}')$$

$$\times B_{4,2}(p_i,q_j)\prod_{i,j}\left(\frac{dp_{i+}}{4\pi}\frac{dq_{j-}}{4\pi}\right)4\pi\delta(\sum p_{i+})4\pi\delta(\sum q_{j-})$$

$$\times C_2(q_j'',p_c'')\prod_j\left(\frac{dq_{j+}''}{4\pi}\right)4\pi\delta(\sum q_{j+}'')$$

$$\times\prod_i\left(\frac{-ie^2}{\mathbf{p}_i^2+\mu^2}\frac{d^2\mathbf{p}_i}{(2\pi)^2}\right)\prod_j\left(\frac{-ie^2}{\mathbf{q}_j^2+\mu^2}\frac{d^2\mathbf{q}_j}{(2\pi)^2}\right)$$

$$\times(2\pi)^2\delta(\sum\mathbf{p}_i-\mathbf{k})(2\pi)^2\delta(\sum\mathbf{q}_j-\mathbf{k}),\quad\text{(A1)}$$

where the subscripts of A, B, and C are numbers of plus or minus indices. We must also sum over all possible photon permutations for the two groups of exchange photons. As mentioned in Sec. II, factors A, B, and C are finite and kinematically decoupled. We can evaluate each of the factors separately.

The first factor,

$$\sum_{\text{(all photon perm.)}}\int A_4(p_a',p')\prod_i\frac{dp_{i-}'}{4\pi}4\pi\delta(\sum p_{i-}'),$$

[30] C. N. Yang, in Proceedings of the Northwestern Symposium, 1970 (unpublished).

can be valuated straightforwardly. Actually, this has been done in the paper of Chang and Ma[16] using a slightly different notation. Interested readers are invited to refer to Sec. V of that paper for details. The result is very simple and independent of the number of photon indices:

$$\sum_{\text{(all perm. for } n \text{ photons)}} \int A_n(p_a',p') \times\prod_{i=1}^{n} \frac{dp_{i-}'}{4\pi} 4\pi\delta(\sum p_{i-}') = \frac{\delta_{aa'}}{m}, \quad \text{(A2)}$$

where a and a' are initial and final helicities of the electron. Similarly, the integral over $C_2(q'',p_c'')$ gives

$$\delta_{cc'}/m. \quad \text{(A3)}$$

Then, the one-bubble amplitude can be written as

$$M^{(1)} = \tfrac{1}{2} s \delta_{aa'} \delta_{bb'} m^{-2} F(s,k), \quad \text{(A4)}$$

with

$$F(s,\mathbf{k}) = \frac{1}{2}\int B_{4,2}(p,q) \times\prod_{ij}\left(\frac{dp_{i+}}{4\pi}\frac{dq_{j-}}{4\pi}\right) 4\pi\delta(\sum p_{i+}) 4\pi\delta(\sum q_{j-}) \times\prod_i \left(\frac{-ie^2}{\mathbf{p}_i^2+\mu^2}\frac{d^2p_i}{(2\pi)^2}\right)\prod_j\left(\frac{-ie^2}{\mathbf{q}_j^2+\mu^2}\frac{d^2\mathbf{q}_j}{(2\pi)^2}\right) \times(2\pi)^2\delta(\sum \mathbf{p}_i-\mathbf{k})(2\pi)^2\delta(\sum \mathbf{q}_j-\mathbf{k}). \quad \text{(A5)}$$

Now, let us evaluate the second-order iteration of the bubble, as shown in Fig. 14(b). According to Eq. (2.17), the amplitude of Fig. 14(b), with photons permuted in all possible ways, consists of the following contributions:

(1) A factor $\delta_{aa'}/m$ from particle a, and a factor $\delta_{cc'}/m$ from particle c.

(2) By the use of

$$\sum_{i=1}^{4}\mathbf{p}_i=\sum_{j=1}^{2}\mathbf{q}_j=\mathbf{k}^{(1)}, \quad \sum_{i=5}^{8}\mathbf{p}_i=\sum_{j=3}^{4}\mathbf{q}_j=\mathbf{k}^{(2)},$$

$$(2\pi)^2\delta^{(2)}(\sum_{i=1}^{8}\mathbf{p}_i-\mathbf{k}) = \int\frac{d^2k^{(1)}}{(2\pi)^2}\frac{d^2k^{(2)}}{(2\pi)^2}(2\pi)^2\delta(\sum_{i=1}^{4}\mathbf{p}_i-\mathbf{k}^{(1)}) \times(2\pi)^2\delta(\sum_{i=5}^{8}\mathbf{p}_i-\mathbf{k}^{(2)})(2\pi)^2\delta(\mathbf{k}^{(1)}+\mathbf{k}^{(2)}-\mathbf{k}), \quad \text{(A6)}$$

the contributions from bubble (1) and bubble (2) are

$$\int B_{4,2}(p_1,\ldots,p_4;q_1,q_2) \times\prod_{i=1}^{4}\prod_{j=1}^{2}\frac{dp_{i+}}{4\pi}\frac{dq_{j-}}{4\pi}4\pi\delta(\sum p_{i+})4\pi\delta(\sum q_{j-}) \times\prod_{i=1}^{4}\frac{-ie^2}{\mathbf{p}_i^2+\mu^2}\frac{d^2p_i}{(2\pi)^2}(2\pi)^2\delta(\sum \mathbf{p}_i-\mathbf{k}^{(1)}) \times\prod_{j=1}^{2}\frac{-ie^2}{\mathbf{q}_j^2+\mu^2}\frac{d^2q_j}{(2\pi)^2}(2\pi)^2\delta(\sum \mathbf{q}_j-\mathbf{k}^{(1)}) = 2F(s,\mathbf{k}^{(1)}) \quad \text{(A7)}$$

and $2F(s,\mathbf{k}^{(2)})$, respectively. (Note that we have included the photon propagators here.)

(3) Since bubbles (1) and (2) are identical, there is a correction factor of $1/2!$ for overcounting.

(4) There is an over-all factor $s/2^{N+1}=\frac{1}{8}s$, $N=2$, in Eq. (2.17). Putting (1)–(4) together, we have

$$M^{(2)} = \tfrac{1}{2}s\delta_{aa'}\delta_{bb'}m^{-2}\frac{1}{2!}\int\frac{d^2k}{(2\pi)^2}(2\pi)^2\delta(\mathbf{k}^{(1)}+\mathbf{k}^{(2)}-\mathbf{k}) \times F(s,\mathbf{k}^{(1)})F(s,\mathbf{k}^{(2)}) = \tfrac{1}{2}s\delta_{aa'}\delta_{bb'}m^{-2}\frac{1}{2!}\int d^2b\, e^{-i\mathbf{k}\cdot\mathbf{b}}[-i\chi(s,\mathbf{b})]^2, \quad \text{(A8)}$$

where

$$-i\chi(s,\mathbf{b}) = \int\frac{d^2k}{(2\pi)^2}e^{i\mathbf{k}\cdot\mathbf{b}}F(s,\mathbf{k}). \quad \text{(A9)}$$

The above result generalizes in an obvious way to N-bubble s-channel iteration, giving

$$M^{(N)}(s,\mathbf{k}) = \tfrac{1}{2}s\delta_{aa'}\delta_{bb'}m^{-2}\frac{1}{N!}\int d^2b \times e^{-i\mathbf{k}\cdot\mathbf{b}}[-i\chi(s,\mathbf{b})]^N. \quad \text{(A10)}$$

Therefore, the summation over all bubbles leads to the eikonal form

$$M(s,\mathbf{k}) = \tfrac{1}{2}s\delta_{aa'}\delta_{bb'}m^{-2}\int d^2b\, e^{-i\mathbf{k}\cdot\mathbf{b}}[e^{-i\chi(s,\mathbf{b})}-1]. \quad \text{(A11)}$$

This is exactly Eq. (5.3) or (5.7).

When more than one kind of connected piece is iterated, the amplitude for N_1 bubbles of one kind, N_2 bubbles of a second kind, etc., is

$$M^{(N_1,N_2,\ldots)}(s,\mathbf{k}) = \tfrac{1}{2}s\delta_{aa'}\delta_{bb'}m^{-2}\frac{1}{N_1!N_2!\cdots}\int d^2b \times e^{-i\mathbf{k}\cdot\mathbf{b}}[-i\chi^{(1)}(s,\mathbf{b})]^{N_1}[-i\chi^{(2)}(s,\mathbf{b})]^{N_2}\cdots, \quad \text{(A12)}$$

where $\chi^{(i)}$ is the eikonal for the ith kind of bubble. Summation over $\{N^i\}$ gives once again Eq. (A11) with

$$\chi(s,\mathbf{b}) = \sum_i \chi^i(s,\mathbf{b}).$$